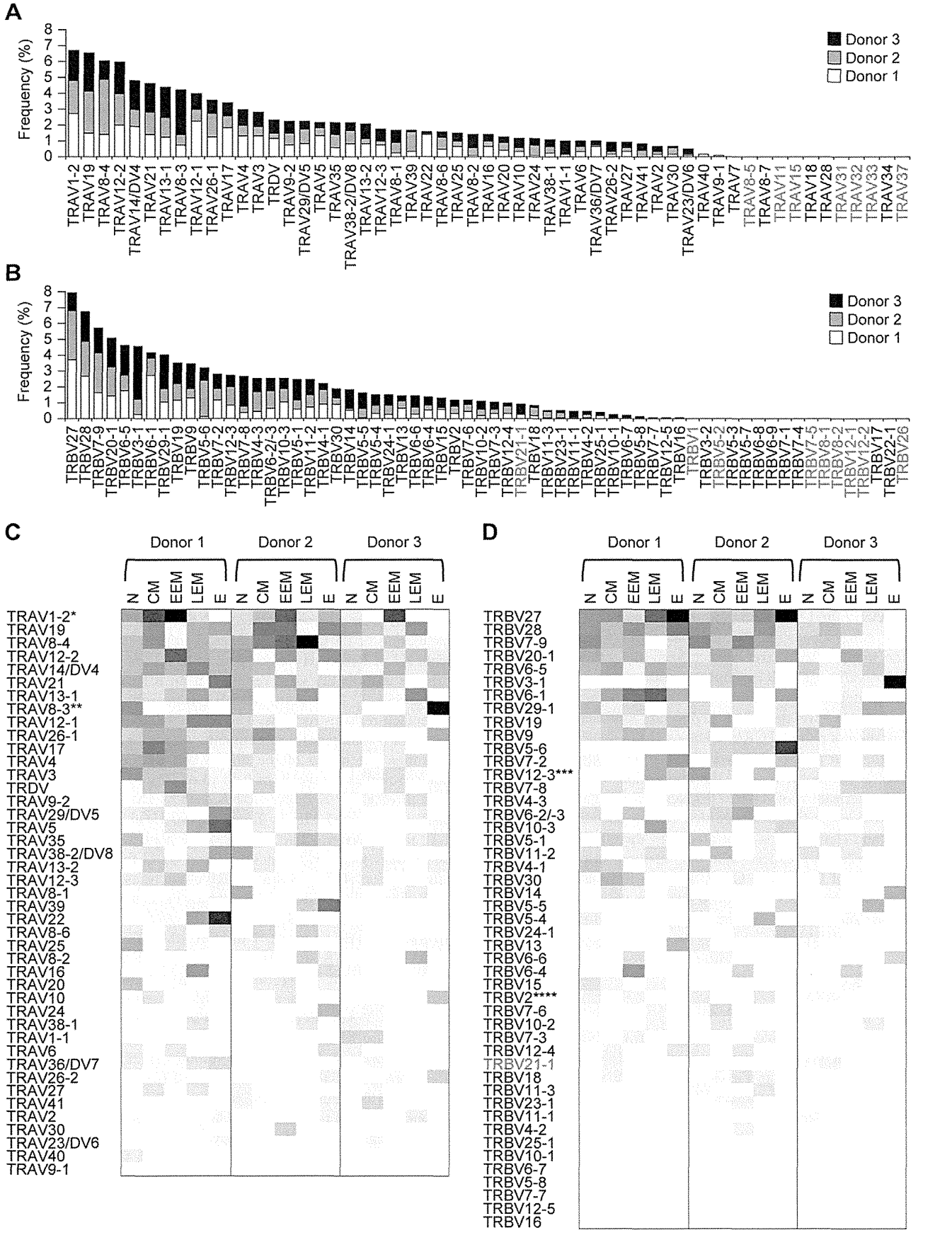
A
Frequency (%)
Donor 3
Donor 2
Donor 1
TRAV1-2
TRAV19
TRAV8-4
TRAV12-2
TRAV14/DV4
TRAV21
TRAV13-1
TRAV8-3
TRAV12-1
TRAV26-1
TRAV17
TRAV4
TRAV3
TRDV
TRAV9-2
TRAV29/DV5
TRAV5
TRAV35
TRAV38-2/DV8
TRAV13-2
TRAV12-3
TRAV8-1
TRAV39
TRAV22
TRAV8-6
TRAV25
TRAV8-2
TRAV16
TRAV20
TRAV10
TRAV24
TRAV38-1
TRAV1-1
TRAV6
TRAV36/DV7
TRAV26-2
TRAV27
TRAV41
TRAV2
TRAV30
TRAV23/DV6
TRAV40
TRAV9-1
TRAV7
TRAV8-5
TRAV8-7
TRAV11
TRAV15
TRAV18
TRAV28
TRAV31
TRAV32
TRAV33
TRAV34
TRAV37
B
Frequency (%)
Donor 3
Donor 2
Donor 1
TRBV27
TRBV28
TRBV7-9
TRBV20-1
TRBV6-5
TRBV3-1
TRBV6-1
TRBV29-1
TRBV19
TRBV9
TRBV5-6
TRBV7-2
TRBV12-3
TRBV7-8
TRBV4-3
TRBV6-2/-3
TRBV10-3
TRBV5-1
TRBV11-2
TRBV4-1
TRBV30
TRBV14
TRBV5-5
TRBV5-4
TRBV24-1
TRBV13
TRBV6-6
TRBV6-4
TRBV15
TRBV2
TRBV7-6
TRBV10-2
TRBV7-3
TRBV12-4
TRBV21-1
TRBV18
TRBV11-3
TRBV23-1
TRBV11-1
TRBV4-2
TRBV25-1
TRBV10-1
TRBV6-7
TRBV5-8
TRBV7-7
TRBV12-5
TRBV16
TRBV1
TRBV3-2
TRBV5-2
TRBV5-3
TRBV5-7
TRBV6-8
TRBV6-9
TRBV7-1
TRBV7-4
TRBV7-5
TRBV8-1
TRBV8-2
TRBV12-1
TRBV12-2
TRBV17
TRBV22-1
TRBV26
C
Donor 1
Donor 2
Donor 3
N
CM
EEM
LEM
E
TRAV1-2*
TRAV19
TRAV8-4
TRAV12-2
TRAV14/DV4
TRAV21
TRAV13-1
TRAV8-3**
TRAV12-1
TRAV26-1
TRAV17
TRAV4
TRAV3
TRDV
TRAV9-2
TRAV29/DV5
TRAV5
TRAV35
TRAV38-2/DV8
TRAV13-2
TRAV12-3
TRAV8-1
TRAV39
TRAV22
TRAV8-6
TRAV25
TRAV8-2
TRAV16
TRAV20
TRAV10
TRAV24
TRAV38-1
TRAV1-1
TRAV6
TRAV36/DV7
TRAV26-2
TRAV27
TRAV41
TRAV2
TRAV30
TRAV23/DV6
TRAV40
TRAV9-1
D
Donor 1
Donor 2
Donor 3
N
CM
EEM
LEM
E
TRBV27
TRBV28
TRBV7-9
TRBV20-1
TRBV6-5
TRBV3-1
TRBV6-1
TRBV29-1
TRBV19
TRBV9
TRBV5-6
TRBV7-2
TRBV12-3***
TRBV7-8
TRBV4-3
TRBV6-2/-3
TRBV10-3
TRBV5-1
TRBV11-2
TRBV4-1
TRBV30
TRBV14
TRBV5-5
TRBV5-4
TRBV24-1
TRBV13
TRBV6-6
TRBV6-4
TRBV15
TRBV2****
TRBV7-6
TRBV10-2
TRBV7-3
TRBV12-4
TRBV21-1
TRBV18
TRBV11-3
TRBV23-1
TRBV11-1
TRBV4-2
TRBV25-1
TRBV10-1
TRBV6-7
TRBV5-8
TRBV7-7
TRBV12-5
TRBV16

Figure 4. TRAV and TRBV usage in CD8+ T-cell subsets among 3 unrelated donors. (A) Frequency of TRAV usage in the 3 donors. (B) Frequency of TRBV usage in the 3 donors. (C-D) TRAV (C) and TRBV (D) usage in $CD8^+$ T-cell subsets among the 3 donors. The same data set used for TIS analysis was used for all analysis of TRAV and TRBV usage. The frequency is proportional to the density of colors: white (low) to black (high). The pseudogenes of TRAV and TRBV are shown in red. N: naive, CM: central memory, EEM: early effector memory, LEM: late effector memory, E: effector. Statistical analysis was performed using the $\chi 2$ and Student' s t test. *: $P<0.05$, EEM>N, EEM>LEM, EEM>E, **: $P<0.05$, N>CM, N>EEM, N>LEM, ***: $P<0.05$, LEM>EEM, ****: $P<0.05$, N>E.
doi:10.1371/journal.pone.0040386.g004

Chimeric TCRs created by the rearrangement of Vδ-Jα has been found in peripheral T-cells of mice and humans, and the heterodimerization of chimeric δα TCR and TCRβ chains can be expressed on the surface of $CD8^+$ T-cells and they recognize antigen presented by antigen-presenting cells [35–37]. We also found that a subset of $CD8^+$ T-cells expressed the chimeric δα TCR chain together with the TCRβ chain. We are not able to know the function of the chimeric δα TCR chain, owing to the limitations of our technology, but the finding of the clonotype showing the identical pair of chimeric δα TCR chain and TCRβ chains in the early effector memory subset suggests that these cells had some function in response to antigen stimulation *in vivo*. These findings suggest that the diversity of human TCRα/β genes may be greater than previously estimated [14].

The expression of TCRα/β chains varied among $CD8^+$ T-cell subsets in the 3 unrelated donors having different HLA-types (except for HLA-A*24:02 type in donor 2 and donor 3), but a finding that about 10~20% of early effector memory cells in all 3 unrelated donors expressed a particular type of TCRα chain carrying a rearrangement of TRAV1-2 and TRAJ33 is interesting from an immunological point of view. Although further study with an increased number of donors will be necessary, a detailed analysis showing the highly conserved CDR3α in rearrangements of TRAV1-2 and TRAJ33 and the preferential usage of the TRBV6 subgroup as its partner may suggest that these early effector memory cells are distinct from the other subsets and recognize various pMHC complexes with some similarity at the level of protein conformation.

In summary, we described herein an unbiased method for amplification of paired TCRα/β chains at the single-cell level. We believe that our method is novel and has the potential for a wide range of applications. Indeed, the application of the method for the characterization of TCRα/β chains in $CD8^+$ T-cell subsets could provide the first evidence that the proportion of TCRα/β identity and clonotypes is associated with the effector function of $CD8^+$ T-cells. We expect that our method using phenotypic classification of $CD8^+$ and $CD4^+$ T-cells will be a useful tool to identify the dynamics of TCRα/β genes in patients with various infectious diseases or tumors and may contribute to the immunotherapy of them.

Materials and Methods

Sample preparation

Human peripheral blood mononuclear cells (PBMCs) were prepared from heparinized peripheral blood from 3 unrelated donors (Table 1), using Ficoll-Paque PLUS (GE Healthcare, Uppsala, Sweden), and stored in liquid nitrogen. Before use, the PBMCs were rested overnight in culture media (RPMI 1640 supplemented with 10% FCS, 100 U/ml MEM-NEAA, 100 U/ml sodium pyruvate, and 200 U/ml recombinant human IL-2). This study was approved by the Kumamoto University Ethical Committee, and written informed consent was obtained from all participants.

Cell staining and single-cell sorting

Surface staining of PBMCs and classification into $CD8^+$ T-cell subsets were performed as described previously [24]. Single cells sorted from each of the $CD8^+$ T-cell subsets by use of a FACSAria equipped with 405-, 488-, and 633-nm lasers and FACSDiva acquisition software (BD Biosciences) were plated into a 96-well plate containing cell lysis buffer (see below).

Single-cell RT-PCR with integrated 5′-RACE and multiplex PCR

The sorted single cells were plated into each well of a 96-well plate with 2 μl of cell lysis buffer containing 1.5 μl of resuspension buffer (Invitrogen), 0.1 μl of lysis enhancer solution (Invitrogen), 0.03 μl of 25 mM dNTPs, 0.1 μl of 40,000U/ml RNase inhibitor, and 0.22 μl of a primer mixture (10 μM concentration of each of hTCR-CA-R2.2, hTCR-CB1-R3.2, and hTCR-CB2-R3 primer) (Table S5). The cells were incubated at 75°C for 10 min and then put on ice immediately. cDNA was synthesized directly from cell lysates by using 6.0 μl of reverse-transcription (RT) solution consisting of 1.2 μl of 5x 1st- strand DNA buffer (Invitrogen), 0.19 μl of 0.1M DTT (Invitrogen), 0.19 μl of RNase inhibitor (NEB), 0.19 μl of SuperScriptIII Reverse Transcriptase (Invitrogen), and 2.33 μl of DEPC-treated H_2O (Invitrogen). RT reactions were performed at 54°C for 60 minutes followed by incubation at 85°C for 5 minutes. Template RNA was digested with 1U of RNase H (Invitrogen) at 37°C for 20 minutes. Extra primers and dNTPs were removed from RT samples by use of a Zymo-Spin™ I-96 Plate (ZYMO Research) according to the manufacturer's instructions. The purified cDNA was incubated at 94°C for 3 minutes and subsequently on ice for at least 2 minutes, and then the tailing of the cDNA was performed with 2 μl of tailing solution consisting of 0.15 μl of 10 mM dGTP (Promega), 0.15 μl of 1M P-K buffer (1M K_2HPO_4, 1M KH_2PO_4; pH7.0), 0.48 μl of 25 mM $MgCl_2$ (Promega), 40 U/μl TdT (Roche), and 1.12 μl of water. The tailing was performed at 37°C for 60 minutes followed by incubation at 65°C for 10 minutes. For amplification of TCRα- and TCRβ-chain transcripts, touch-down PCR (first-round PCR) was performed in 25 μl of 2x primeSTAR GC buffer (TaKaRa), 4 μl of 2.5 mM dNTPs (TaKaRa), 1 μl of 10 μM Oligo-dc-adaptor2, 1 μl of 10 μM hTCR-CA-R7, 1 μl of 10 μM hTCR-CB1-R9, 0.625 U of PrimeSTAR (TaKaRa), and 5.75 μl of water, using the following conditions: 1) 96°C for 2 minutes, 2) 3 cycles of 96°C for 15 seconds and 72°C for 2 minutes, 3) 3 cycles of 96°C for 15 seconds, 69°C for 15 seconds, and 72°C for 1.5 minutes, 4) 3 cycles of 96°C for 15 seconds, 66°C for 15 seconds, and 72°C for 1.5 minutes, 5) 26 cycles of 96°C for 15 seconds, 63°C for 15 seconds, and 72°C for 1.5 minutes. Using 1 μl of a 1:20 dilution of the first-round PCR reactions, a nested second PCR was performed in a 20 μl reaction mixture consisting of 10 μl of 2x PrimeSTAR GC buffer (TaKaRa), 1.6 μl of 2.5 mM dNTPs (TaKaRa), 0.1 μl of 2.5 U/μl PrimeSTAR (TaKaRa), 6.66 μl of water, 0.32 μl of 10 μM AP2, and 0.32 μl of 10 μM reverse primer corresponding to the TCR constant region (hTCR-CA-R9 for TCRα chain and hTCR-CB1-R6 for TCRβ chain). The PCR conditions were as follow: 1) 96°C for 2 minutes, 2) 35 cycles of 96°C for 15 seconds, 58°C for 30

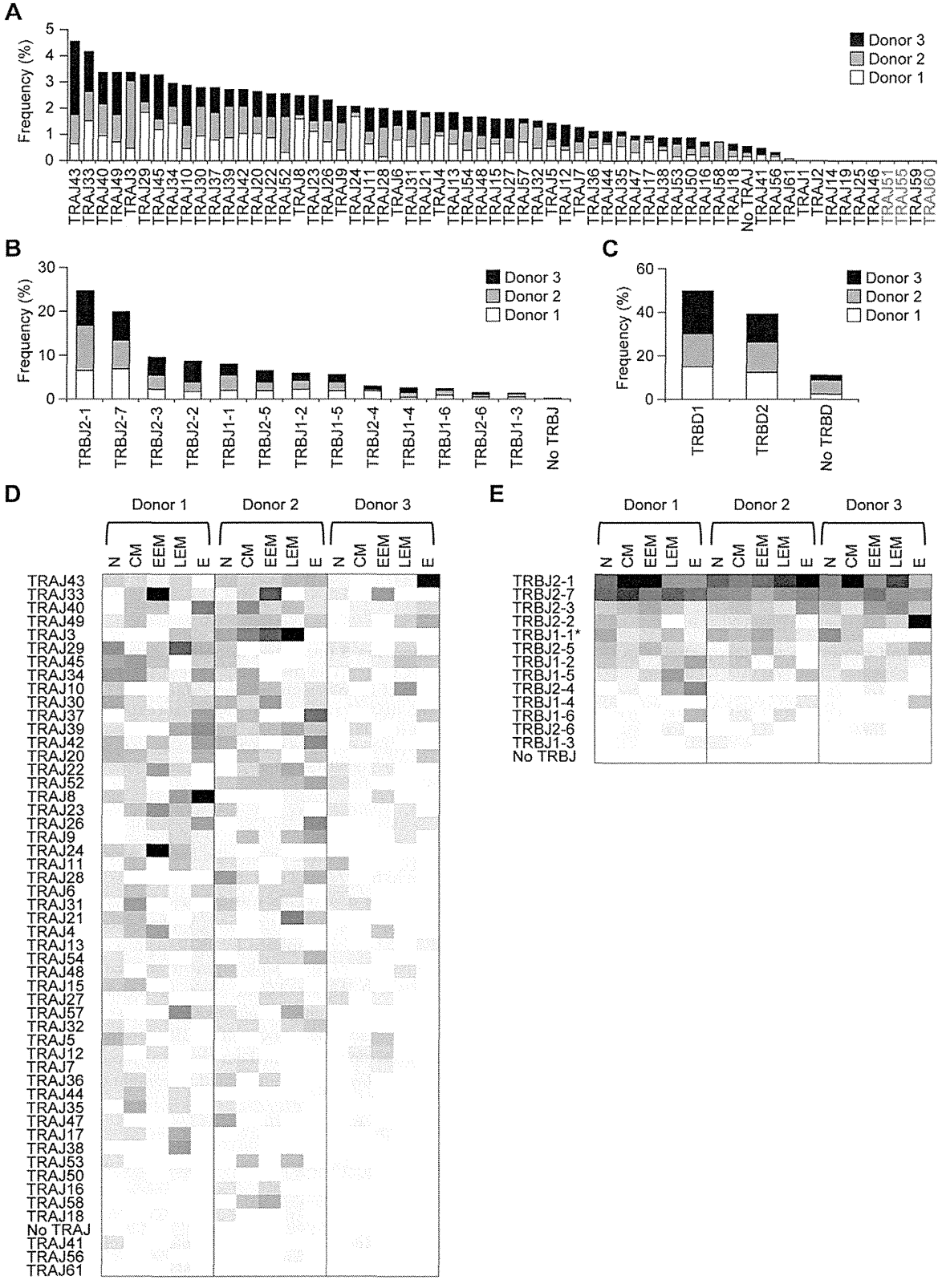

Figure 5. TRAJ, TRBJ, and TRBD usage in CD8+ T-cell subsets among the 3 unrelated donors. (A) Frequency of TRAJ usage in the 3 donors. (B) Frequency of TRBJ usage in the same donors. (C) Frequency of TRBD usage in the 3 donors. (D) TRAJ usage in CD8+ T-cell subsets among the 3 donors. (E) TRBJ usage in CD8+ T-cell subsets among the same donors. The frequency is proportional to the density of colors from white (low) to black (high). The pseudotypes of TRAJ and TRBJ are shown in red. Statistical analysis was performed using the $\chi 2$ and Student's t test. *: $P<0.05$, N>EEM, N>E.

doi:10.1371/journal.pone.0040386.g005

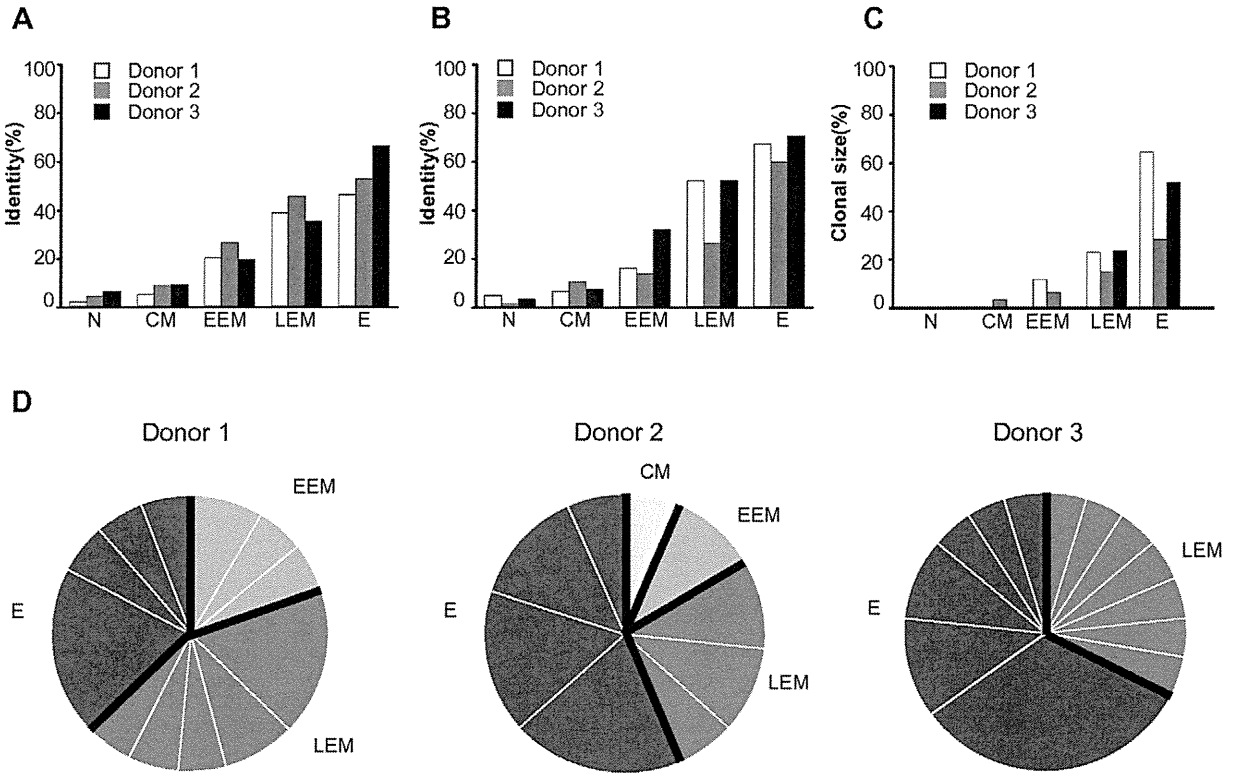

Figure 6. Identity and clonotype of TCRα/β chains in CD8+ T-cell subsets among the 3 unrelated donors. A data set not including samples showing germline transcripts was used for the analysis (1,207 and 1,540 reads for TCRα and TCRβ chains, respectively). (A) Frequency of TCRα chain identity in CD8+ T-cell subsets. The identity was defined as more than 2 appearances of samples with the identical usage of TRAV, TRAJ, and CDR3α. (B) Frequency of identical TCRα and β chains in CD8+ T-cell subsets. The identity was defined as more than 2 appearances of samples with the identical usage of TRBV, TRBD, TRBJ, and CDR3β. (C) Frequency of paired TCRα/β clonotype in CD8+ T-cell subsets. The percentage was measured by using a data set obtained from 901 paired TCRα/β sequence reads. The clonotype was defined by the more than 2 appearances of samples showing identical TCRα/β chains. (D) Proportion of TCRα/β clonotypes in CD8+ T-cell subsets among the 3 unrelated donors. The TCRα/β clonotypes identified in "C" were discriminated by type and proportion (see Table S4).
doi:10.1371/journal.pone.0040386.g006

seconds, and 72°C for 1 minute, and 3) 72°C for 3 minutes. Multiplex PCR was also performed with 2.5 μl of the first-round PCR product, 10 μl of Taq colorless buffer (Promega), 3 μl of 25 mM $MgCl_2$ (Promega), 4 μl 2.5 mM dNTPs (Promega), 50 U of Taq DNA polymerase (Promega), 0.5 μl of a 10 μM oligonucleotide mixture, containing either 1 of 54 TRAV forward primers or 1 of 65 TRBV forward primers, and 0.32 μl of the 10 μM reverse primer for the TCR constant region under the following conditions: 1) 96°C for 2 minutes, 2) 35 cycles of 96°C for 15 seconds, 57°C for 30 seconds, and 72°C for 1 minute, and 3) 72°C for 3 minutes.

Sequencing and data analysis

One microliter of the PCR products was treated with 0.2 μl of ExoSAP-IT (usb) at 37°C for 15 minutes and subsequently at 80°C for 15 minutes. Sequencing reactions were performed in a 9 μl of reaction mixture consisting of 1 μl of the ExoSAP-IT-treated PCR products, 0.15 μl of 10 μM TCR reverse primer (hTCR-alpha-1st or hTCR-alpha-1st), 1.5 μl of 5x sequencing buffer, 1 μl of BigDye® Terminator v3.1, and 5.35 μl of water. The mixture was incubated at 96°C for 1 minutes followed by 25 cycles of 96°C for 10 seconds and 62°C for 1 minute. The sequences were determined with 3500 and 3500xL Genetic Analyzer (Applied Biosystem, USA). The repertoire of TCRα and TCRβ chains was analyzed by the IMGT/V-QUEST search tool (http://www.imgt.org/IMGT_vquest/vquest?livret = 0&Option = humanTcR), and germ-line transcripts were identified by searching against the human genome sequences (BLAST search: http://blast.ncbi.nlm.nih.gov/).

The presence of dual TCRs was detected by sequence analysis with Sequence Scanner v1.0 software (Applied Biosystem, USA). Individual TCRs were amplified by PCR with a single forward primer designed for each variable segment and the TCR reverse primer (hTCR-CA-R9 for TCRα chain or hTCR-CB1-R6 for TCRβ chain). Sequencing reactions and data analysis were performed as described above. If PCR products show the sequences of two alpha and one beta chains or those of one alpha and two beta chains, a cell is evaluated to contain dual TCR.

Supporting Information

Figure S1 Non-canonical rearrangement of the alpha chain.
(TIF)

Figure S2 Conservation of CDR3α amino acid sequences created by TRAV1-2 and TRAJ31 rearrangements in early effector memory subset. CDR3α amino acid sequences created by TRAV1-2 and TRAJ31 rearrangements were identified by IMGT/V-Quest tool, and the conservation was analyzed by Multiple Align Show (http://www.bioinformatics.org/SMS/multi_align.html). Amino acid sequences having 100% of identity and 50% of similarity are shown in black and dark gray, respectively.
(TIF)

Table S1 Nucleotide sequences of TCRα and β used in this study.
(XLSX)

Table S2 TCR usage and amino acid sequence of CDR3 region. #: Frame shift, ** Stop codon
(XLSX)

Table S3 Characterization of early effector memory cells carrying rearrangements between TRAV1-2 and TRAJ33. #: Frame shift, ** Stop codon
(DOCX)

Table S4 Characterization of TCRα/β clonotypes in CD8+ T-cell subsets.
(DOCX)

Table S5 Primer sequences for 5′-RACE and multiplex PCR methods for amplification of human TCRα/β chains.
(DOCX)

Acknowledgments

The authors thank Megumi Shibuya for technical assistance and Sachiko Sakai for secretarial assistance.

Author Contributions

Conceived and designed the experiments: MT MS AM. Performed the experiments: XS MS YS TO EK HK. Analyzed the data: XS MS TC TN MT. Wrote the paper: MS MT.

References

1. Guidotti LG, Chisari FV (1996) To kill or to cure: options in host defense against viral infection. Curr Opin Immunol 8: 478–483.
2. Levy JA, Mackewicz CE, Barker E (1996) Controlling HIV pathogenesis: the role of the noncytotoxic anti-HIV response of CD8+ T cells. Immunol Today 17: 217–224.
3. Robbins PF, Dudley ME, Wunderlich J, El-Gamil M, Li YF, et al. (2004) Cutting edge: persistence of transferred lymphocyte clonotypes correlates with cancer regression in patients receiving cell transfer therapy. J Immunol 173: 7125–7130.
4. Kaech SM, Ahmed R (2001) Memory CD8+ T cell differentiation: initial antigen encounter triggers a developmental program in naive cells. Nat Immunol 2: 415–422.
5. van Stipdonk MJ, Lemmens EE, Schoenberger SP (2001) Naive CTLs require a single brief period of antigenic stimulation for clonal expansion and differentiation. Nat Immunol 2: 423–429.
6. Tomiyama H, Matsuda T, Takiguchi M (2002) Differentiation of human CD8(+) T cells from a memory to memory/effector phenotype. J Immunol 168: 5538–5550.
7. Bassing CH, Swat W, Alt FW (2002) The mechanism and regulation of chromosomal V(D)J recombination. Cell 109 Suppl: S45–55.
8. Davis MM, Bjorkman PJ (1988) T-cell antigen receptor genes and T-cell recognition. Nature 334: 395–402.
9. Gellert M (1992) Molecular analysis of V(D)J recombination. Annu Rev Genet 26: 425–446.
10. Gellert M (2002) V(D)J recombination: RAG proteins, repair factors, and regulation. Annu Rev Biochem 71: 101–132.
11. Jung D, Alt FW (2004) Unraveling V(D)J recombination; insights into gene regulation. Cell 116: 299–311.
12. Gorski J, Yassai M, Zhu X, Kissela B, Kissella B, et al. (1994) Circulating T cell repertoire complexity in normal individuals and bone marrow recipients analyzed by CDR3 size spectratyping. Correlation with immune status. J Immunol 152: 5109–5119.
13. Pannetier C, Cochet M, Darche S, Casrouge A, Zoller M, et al. (1993) The sizes of the CDR3 hypervariable regions of the murine T-cell receptor beta chains vary as a function of the recombined germ-line segments. Proc Natl Acad Sci U S A 90: 4319–4323.
14. Robins HS, Campregher PV, Srivastava SK, Wacher A, Turtle CJ, et al. (2009) Comprehensive assessment of T-cell receptor beta-chain diversity in alphabeta T cells. Blood 114: 4099–4107.
15. Freeman JD, Warren RL, Webb JR, Nelson BH, Holt RA (2009) Profiling the T-cell receptor beta-chain repertoire by massively parallel sequencing. Genome Res 19: 1817–1824.
16. Robins HS, Srivastava SK, Campregher PV, Turtle CJ, Andriesen J, et al. (2010) Overlap and effective size of the human CD8+ T cell receptor repertoire. Sci Transl Med 2: 47ra64.
17. Shendure J, Ji H (2008) Next-generation DNA sequencing. Nat Biotechnol 26: 1135–1145.
18. Sherwood AM, Desmarais C, Livingston RJ, Andriesen J, Haussler M, et al. (2011) Deep sequencing of the human TCRgamma and TCRbeta repertoires suggests that TCRbeta rearranges after alphabeta and gammadelta T cell commitment. Sci Transl Med 3: 90ra61.
19. Dash P, McClaren JL, Oguin TH 3rd Rothwell W, Todd B, et al. (2011) Paired analysis of TCRalpha and TCRbeta chains at the single-cell level in mice. J Clin Invest 121: 288–295.
20. Hamrouni A, Aublin A, Guillaume P, Maryanski JL (2003) T cell receptor gene rearrangement lineage analysis reveals clues for the origin of highly restricted antigen-specific repertoires. J Exp Med 197: 601–614.
21. Ozawa T, Tajiri K, Kishi H, Muraguchi A (2008) Comprehensive analysis of the functional TCR repertoire at the single-cell level. Biochem Biophys Res Commun 367: 820–825.
22. Frohman MA, Dush MK, Martin GR (1988) Rapid production of full-length cDNAs from rare transcripts: amplification using a single gene-specific oligonucleotide primer. Proc Natl Acad Sci U S A 85: 8998–9002.
23. Edwards MC, Gibbs RA (1994) Multiplex PCR: advantages, development, and applications. PCR Methods Appl 3: S65–75.
24. Takata H, Takiguchi M (2006) Three memory subsets of human CD8+ T cells differently expressing three cytolytic effector molecules. J Immunol 177: 4330–4340.
25. Sikes ML, Gomez RJ, Song J, Oltz EM (1998) A developmental stage-specific promoter directs germline transcription of D beta J beta gene segments in precursor T lymphocytes. J Immunol 161: 1399–1405.
26. Villey I, Quartier P, Selz F, de Villartay JP (1997) Germ-line transcription and methylation status of the TCR-J alpha locus in its accessible configuration. Eur J Immunol 27: 1619–1625.
27. Anderson SJ, Chou HS, Loh DY (1988) A conserved sequence in the T-cell receptor beta-chain promoter region. Proc Natl Acad Sci U S A 85: 3551–3554.
28. Deng X, Sun GR, Zheng Q, Li Y (1998) Characterization of human TCR Vbeta gene promoter. Role of the dodecamer motif in promoter activity. J Biol Chem 273: 23709–23715.
29. Yang S, Cohen CJ, Peng PD, Zhao Y, Cassard L, et al. (2008) Development of optimal bicistronic lentiviral vectors facilitates high-level TCR gene expression and robust tumor cell recognition. Gene Ther 15: 1411–1423.
30. Inlay M, Xu Y (2003) Epigenetic regulation of antigen receptor rearrangement. Clin Immunol 109: 29–36.
31. Padovan E, Casorati G, Dellabona P, Giachino C, Lanzavecchia A (1995) Dual receptor T-cells. Implications for alloreactivity and autoimmunity. Ann N Y Acad Sci 756: 66–70.
32. Singh N, Bergman Y, Cedar H, Chess A (2003) Biallelic germline transcription at the kappa immunoglobulin locus. J Exp Med 197: 743–750.
33. Sleckman BP, Gorman JR, Alt FW (1996) Accessibility control of antigen-receptor variable-region gene assembly: role of cis-acting elements. Annu Rev Immunol 14: 459–481.
34. Schlissel MS, Baltimore D (1989) Activation of immunoglobulin kappa gene rearrangement correlates with induction of germline kappa gene transcription. Cell 58: 1001–1007.
35. Kobayashi Y, Tycko B, Soreng AL, Sklar J (1991) Transrearrangements between antigen receptor genes in normal human lymphoid tissues and in ataxia telangiectasia. J Immunol 147: 3201–3209.
36. Miossec C, Faure F, Ferradini L, Roman-Roman S, Jitsukawa S, et al. (1990) Further analysis of the T cell receptor gamma/delta+ peripheral lymphocyte subset. The V delta 1 gene segment is expressed with either C alpha or C delta. J Exp Med 171: 1171–1188.
37. Ueno T, Tomiyama H, Fujiwara M, Oka S, Takiguchi M (2003) HLA class I-restricted recognition of an HIV-derived epitope peptide by a human T cell receptor alpha chain having a Vdelta1 variable segment. Eur J Immunol 33: 2910–2916.

Biochemical and Biophysical Research Communications 422 (2012) 245–249

Contents lists available at SciVerse ScienceDirect

Biochemical and Biophysical Research Communications

journal homepage: www.elsevier.com/locate/ybbrc

The binding affinity of a soluble TCR-Fc fusion protein is significantly improved by crosslinkage with an anti-Cβ antibody

Tatsuhiko Ozawa [a], Masae Horii [a], Eiji Kobayashi [a], Aishun Jin [a,b], Hiroyuki Kishi [a,*], Atsushi Muraguchi [a]

[a] Department of Immunology, Graduate School of Medicine and Pharmaceutical Sciences, University of Toyama, 2630 Sugitani, Toyama 930-0194, Japan
[b] Department of Immunology, College of Basic Medical Sciences, Harbin Medical University, 157 Baojian Road, Nangang District, Harbin 150081, China

ARTICLE INFO

Article history:
Received 23 April 2012
Available online 1 May 2012

Keywords:
Soluble form of the TCR
Affinity
Anti-Cβ antibody

ABSTRACT

The identification and cloning of tumor antigen-specific T cell receptors (TCRs) and the production of the soluble form of the TCR (sTCR) contributed to the development of diagnostic and therapeutic tools for cancer. Recently, several groups have reported the development of technologies for the production of sTCRs. The native sTCR has a very low binding affinity for the antigenic peptide/MHC (p/MHC) complex. In this study, we established a technology to produce high affinity, functional sTCRs. We generated a novel sTCR-Fc fusion protein composed of the TCR V and C regions of the TCR linked to the immunoglobulin (Ig) Fc region. A Western blot analysis revealed that the molecular weight of the fusion protein was approximately 60 kDa under reducing conditions and approximately 100–200 kDa under non-reducing conditions. ELISAs using various antibodies showed that the structure of each domain of the TCR-Fc protein was intact. The TCR-Fc protein immobilized by an anti-Cβ antibody effectively bound to a p/MHC tetramer. An SPR analysis showed that the TCR-Fc protein had a low binding affinity (*KD*; 1.1×10^{-5} M) to the p/MHC monomer. Interestingly, when the TCR-Fc protein was pre-incubated with an anti-Cβ antibody, its binding affinity for p/MHC increased by 5-fold (2.2×10^{-6} M). We demonstrated a novel method for constructing a functional soluble TCR using the Ig Fc region and showed that the binding affinity of the functional sTCR-Fc was markedly increased by an anti-Cβ antibody, which is probably due to the stabilization of the Vα/Vβ region of the TCR. These findings provide new insights into the binding of sTCRs to p/MHCs and will hopefully be instrumental in establishing functional sTCR as a diagnostic and therapeutic tool for cancer.

1. Introduction

T cell receptors (TCRs) are antigen recognition molecules that are expressed on the surface of T cells. They specifically recognize the antigenic peptide that is presented by the major histocompatibility complex (p/MHC) [1,2]. In tumor immunity, the tumor cells or their antigens are ingested by antigen presenting cells (APCs). The tumor antigens (TAs) are then processed inside the APCs, and the peptides derived from these antigens are displayed on class I MHC molecules, which are recognized by $CD8^+$ T cells. APCs express costimulatory molecules that provide the signals necessary for the differentiation of $CD8^+$ T cells into anti-tumor cytotoxic T lymphocytes (CTLs), which kill tumor cells [3].

The identification of TCRs that specifically recognize the TA-specific p/MHC complex is extremely valuable for developing tools for tumor diagnosis or TCR therapy. However, the identification of TA-specific TCRs is difficult because the establishment of TA-specific T cell clones entails large amounts of time, money, and labor for only a few clones. Nevertheless, many groups have been successful in establishing TA-specific T cell clones and analyzing the TCR genes and their properties, including their affinity and binding capacity for p/MHC.

Because the TCR is a transmembrane protein, it is necessary to generate a soluble form (sTCR) for its application as a diagnostic and therapeutic tool for cancer [4–6]. Thus, many investigators have constructed sTCRs using various methods and have characterized their various functions [7–17]. The results show that the affinity (*KD* value) of the wild-type soluble form of p/MHC is very low compared to that of antibodies, ranging from 1 to 100×10^{-6} M by SPR-based assays [1,18,19]. Specifically, the dissociation rate of TCRs is very fast (k_d, $1–10 \times 10^{-2}\ s^{-1}$) compared to antibodies (k_d, $1–100 \times 10^{-5}\ s^{-1}$), which leads to the formation of an unstable complex between the soluble TCR and the antigenic p/MHC. To increase the binding affinity, the CDR3 of the TCR V region has been optimized by amino acid replacements [20–22]. However, it is difficult to routinely perform optimal amino acid replacements.

In this study, to improve the sTCR affinity for p/MHC, we constructed a novel sTCR by removing the transmembrane and cytoplasmic domains of a TCR derived from the OT-1 TCR and

* Corresponding author. Fax: +81 76 434 5019.
E-mail address: immkishi@med.u-toyama.ac.jp (H. Kishi).

0006-291X/$ - see front matter © 2012 Elsevier Inc. All rights reserved.
http://dx.doi.org/10.1016/j.bbrc.2012.04.134

directly fusing the extracellular portion of the TCR with the Ig Fc region. The resulting sTCR-Fc bound to the p/MHC complex with an affinity of 10×10^{-6} M. Surprisingly, the binding affinity, which was determined by an SPR analysis, was increased by 5-fold by crosslinking the sTCR-Fc with an anti-Cβ antibody. We found that this profound increase in affinity was due to a decrease in the k_d of the sTCR. Additionally, the sTCR-Fc bound to the p/MHC tetramer in an ELISA in the presence of an anti-Cβ antibody. Our data indicate that the binding affinity of an sTCR-Fc is easily improved by adding an anti-Cβ antibody, which may promote its use as a diagnostic or therapeutic tool for cancer.

2. Material and methods

2.1. Ethics statement

The protocols for the animal experiments were approved by the Committee on Animal Experiments at the University of Toyama.

2.2. Antibodies and peptide MHC

In this study, we used an anti-mouse TCR Cβ (anti-Cβ) antibody (H57–597, eBioscience), a PE-labeled anti-Cβ antibody (eBioscience), an anti-mouse Vα2 antibody (eBioscience), a PE-labeled anti-mouse Vα2 antibody (eBioscience), an anti-human IgG Fc (anti-Fc) antibody (MP Biomedicals), a biotinylated anti-mouse Vβ5.1, 5.2 antibody (BD Bioscience), PE-labeled streptavidin (BD Bioscience), the alkaline phosphatase conjugate of the anti-IgG antibody (Sigma), the PE-labeled T-select H-2K^b OVA tetramer-SIINFEKL (OVA-p/MHC tetramer; MBL), and the biotinylated H-2K^b OVA monomer-SIINFEKL (OVA-p/MHC monomer; MBL). We also used the PE-labeled T-Select H-2K^b β-galactosidase tetramer-DAPIYTNV (β-gal-p/MHC tetramer; MBL) and the biotinylated H-2K^b β-galactosidase monomer-DAPIYTNV (β-gal-p/MHC monomer; MBL) as irrelevant controls.

2.3. Generation of OT-1 TCR-Fc constructs

OT-1 TCR transgenic mice whose transgene encoded TCR that recognized the OVA-derived peptide (SIINFEKL) in the presence of the MHC I allele H-2K^b [23] were obtained from The Jackson Laboratory. To generate OT-1 αTCR-Fc and OT-1 βTCR-Fc expression vectors, spleen cells were prepared from the OT-1 TCR transgenic mouse and the OT-1 TCR Vα/Cα and the OT-1 TCR Vβ/Cβ cDNAs were amplified by reverse transcription and polymerase chain reaction (RT-PCR) with primer sets for Vα + Cα (5′-CTCTAACGCGT CGACTCGTGATCGACCATGGACAAGATTCTGAC-3′ and 5′-ATTCTACG CGGATCCGCGCTTACTGACCAGCTTGACATCACAGG-3′) and for Vβ + Cβ (5′-CTCTAACGCGTCGACTCGTGATCGACCATGTCTAACACTG TCCT-3′ and 5′-ATTCTACGCGGATCCGCGCTTACTCACCGAGGTAAAG CCACAGT-3′). Both PCR products were digested by the restriction enzymes *Sal*I and *Bam*HI and were inserted into *Sal*I and *Bam*HI digested expression vectors that contained the human Ig Fc cDNA, including the hinge region and the CH2 and CH3 regions.

2.4. Production and purification of OT-1 TCR-Fc

We co-transfected CHO-S cells (Invitrogen) with both the OT-1 αTCR-Fc and OT-1 βTCR-Fc expression vectors using the FreeStyle™ MAX CHO Expression System (Invitrogen) for one week, collected the supernatant from the cultured cells, and then purified the OT-1 TCR-Fc using a protein G column (GE Healthcare). We purified α/β heterodimer of OT-1 TCR-Fc by Cβ and Vα2 affinity chromatography on Sepharose coupled with anti-Cβ and anti-Vα2 antibody, respectively, which were generated using NHS-activated Sepharose 4 Fast Flow (GE Healthcare) according to the manufacturer's instructions. First, we purified 1 mg of protein G column-purified OT-1 TCR-Fc protein using Cβ affinity chromatography. After elution, we purified the protein using Vα2 affinity chromatography by AKTA prime plus system (GE Healthcare) according to the manufacturer's instructions. To determine the concentration of the purified OT-1 TCR-Fc protein, the OT-1 TCR-Fc protein was captured with an anti-Fc antibody and detected with an alkaline phosphatase conjugate of an anti-IgG antibody. Concentrations of the OT-1 TCR-Fc protein were estimated based on a comparison to control IgG1 antibodies. To determine the purity of α/β heterodimer, we calculated the purity by comparing the purified protein to the control single-chain TCR protein [15] that consists of 100% Vα/Vβ/Cβ region of OT-1 TCR by sandwich ELISA with anti-Cβ and anti-Vα2 antibody.

2.5. ELISA and surface plasmon resonance (SPR) analysis

Black MaxiSorp FluoroNunc™ modules and plates (Nunc) were coated with 50 μl well^{-1} of 2.5 μg ml^{-1} of the anti-Cβ antibody or the anti-Fc antibody in phosphate-buffered saline (PBS) and then blocked with 3% bovine serum albumin in PBS. After washing, 5 nM of the OT-1 TCR-Fc was added to the plate and incubated for 1 h at room temperature. The binding of the OT-1 TCR-Fc to the coated antibody was detected using the OVA-p/MHC tetramer. As a negative control, a similar analysis was also performed using a β-gal-p/MHC tetramer. The PE fluorescence intensity was measured using an excitation wavelength of 544 nm and an emission wavelength of 590 nm with a FLUOstar OPTIMA fluorescence microplate reader (BMG LABTECH), according to the manufacturer's instructions.

Surface plasmon resonance analysis was performed with a Biacore 2000 instrument (Biacore AB, Uppsala, Sweden) in HBS-N running buffer containing 0.05% Tween 20 at 25 °C. The OVA-p/MHC monomer was immobilized to the surface of an SA sensor chip (GE Healthcare), with final immobilization levels of approximately 5000 RU, according to the manufacturer's instructions. For the kinetic measurements, 200 nM of the OT-1 TCR-Fc in the absence or presence of 33 nM of the anti-Cβ antibody was injected into the HBS-N running buffer, containing 0.05% Tween-20, at flow rates of 20 μl min^{-1} with 3 min for association and 15 min for dissociation. Similarly, 100, 50, 25, 12.5, or 0 nM of the OT-1 TCR-Fc in the absence or presence of 16.5, 8.3, 4.1, 2.1, or 0 nM of the anti-Cβ antibody was injected. As negative controls, a similar analysis was performed using the β-gal-p/MHC monomer. The binding affinity (*KD*) values were calculated after subtracting the background binding to a control flow cell using the bivalent binding model for the kinetic analysis with the BIAevaluation 4.1 software (Biacore AB). For the calculation, we used the corrected concentration of the OT-1 TCR-Fc protein according to the purity of α/β heterodimer.

3. Results

3.1. Generation and characterization of soluble TCR proteins

We designed and constructed four different types of sTCRs: (1) scFV-TCR, (2) sVC-TCR, (3) scTCR-Fc, and (4) sTCR-Fc (Supplementary Fig. 1). We found that the scFV-TCR protein was easily produced by transfecting the expression vector into *Escherichia coli* and purifying the proteins from inclusion bodies, but an SPR analysis showed no or extremely low binding affinity of this protein to the peptide/MHC (data not shown). We could not produce sufficient amounts of the sVC-TCR and scTCR-Fc protein for unknown reasons, although we tried various transfection systems (data not

shown). We were able to produce the sTCR-Fc fusion protein using CHO-S cells.

We constructed an Fc-fusion protein with an OT-1 TCR that recognizes an OVA-derived peptide (SIINFEKL) [23]. The TCR portion of this fusion protein comprises the TCR Vα/Cα region and the Vβ/Cβ region. The transmembrane and cytoplasmic domains of Cα or Cβ were removed by truncating them at the fifth amino acid residue of the TCR located downstream of the last cysteine residue and upstream of the transmembrane domain. The Cα and Cβ portions of the OT-1 TCR were linked directly to the Fc portion of a human IgG1 chain that included a hinge region. The cysteine residues in the hinge region were intact, which allowed appropriate disulfide bonding of the H chain regions, and thus the OT-1 TCR-Fc protein was produced as a dimer with a covalent linkage.

To characterize the OT-1 TCR-Fc protein, the purified protein was subjected to SDS–PAGE and Western blot analysis (Fig. 1A). Under reducing conditions, proteins of approximately 60 kDa were detected, which is consistent with the calculated molecular mass for this protein based on its predicted amino acid sequence. Under non-reducing conditions, proteins of approximately 100–200 kDa were detected. The apparent shift in molecular mass of the OT-1 TCR-Fc protein under reducing vs. non-reducing conditions indicated that there were disulfide bonds between the H chains of cysteine residues. Therefore, the OT-1 TCR-Fc proteins formed a dimeric structure.

To determine whether the structure of each domain (Vα, Vβ, or Cβ) was intact, we performed a sandwich enzyme-linked immunosorbent assay (ELISA). When the OT-1 TCR-Fc protein was immobilized by an anti-Fc antibody, antibodies specific to Vβ5.1/5.2, Cβ, and Vα2 bound to the OT-1 TCR-Fc proteins (Fig. 1B). Although the OT-1 TCR-Fc proteins were covalently linked as a dimer (Fig. 1A), dimers formed not only as α/β heterodimers, but also as α/α or β/β homodimers. To determine whether the purified OT-1 TCR-Fc protein contained the α/β heterodimer form, we pre-coated another sandwich ELISA. When the OT-1 TCR-Fc protein was immobilized by an anti-Cβ antibody, the Vα2 of the OT-1 TCR-Fc protein was detected (Fig. 1C). Similarly, when the OT-1 TCR-Fc was immobilized by an anti-Vα2 antibody, the Cβ of the OT-1 TCR-Fc protein was detected (Fig. 1C). These results suggest that the structures of each domain were intact. Next, we determined the purity of α/β heterodimer of OT-1 TCR-Fc protein using sandwich ELISA. The purity of pre- and post-purification was estimated to be approximately 15% and 45%, respectively (Supplementary Fig. 2).

3.2. p/MHC binding to the OT-1 TCR-Fc protein

The OT-1 TCR specifically recognizes the OVA (SIINFEKL)-peptide and the MHC complex (OVA-p/MHC). To determine whether the OT-1 TCR-Fc protein recognized the OVA-p/MHC, we used a pre-coated ELISA. The OT-1 TCR-Fc was incubated with an

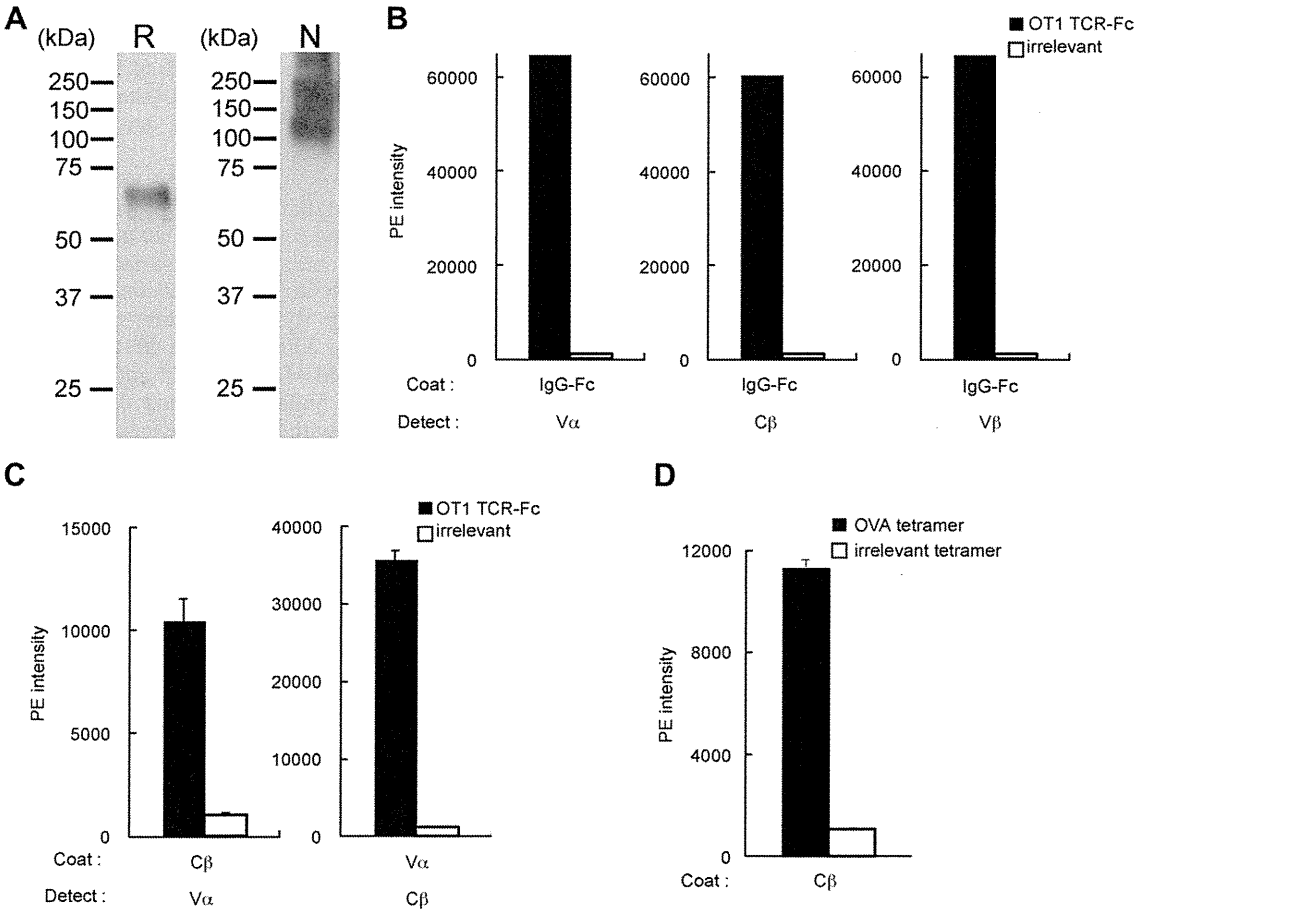

Fig. 1. Characterization of the OT-1 TCR-Fc protein. (A) The examination of the dimer form of the OT-1 TCR-Fc protein. The OT-1 TCR-Fc protein was separated by SDS–PAGE under either reducing (R) or non-reducing (N) conditions. The OT-1 TCR-Fc protein was detected by Western blotting using a horseradish peroxidase-conjugated anti-Fc antibody. (B) The examination of the OT-1 TCR-Fc domains. The OT-1 TCR-Fc protein or an IgG (control) was immobilized by an anti-Fc antibody, and the conformation of the Vα, Cβ, and Vβ domains was assessed using PE-labeled antibodies to Vα (left), Cβ (middle), or Vβ (right). (C) The examination of the α/β heterodimer form of the OT-1 TCR-Fc protein. The OT-1 TCR-Fc protein or an IgG (control) was immobilized by an anti-Cβ (left) or anti-Vα antibody (right), and Vα and Cβ were detected using a PE-labeled anti-Vα or anti-Cβ antibody, respectively. (D) The reactivity of the OT-1 TCR-Fc protein with p/MHC. The OT-1 TCR-Fc protein was immobilized by an anti-Cβ and its reactivity to the OVA-p/MHC tetramer or a β-gal-p/MHC tetramer (control) was assessed by incubation with their PE-conjugates. (B–D) The Y-axis shows the fluorescence intensity. All of the data represent the mean ± SD.

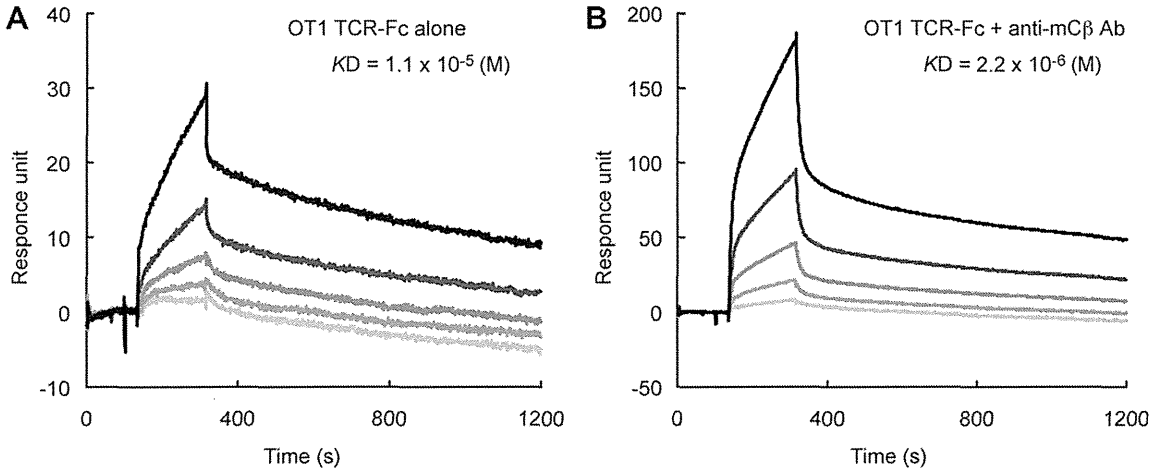

Fig. 2. Surface plasmon resonance (SPR) analysis of the OT-1 TCR-Fc protein. SPR measurements of individual analytes are shown: the OT-1 TCR-Fc protein alone (A), and the OT-1 TCR-Fc protein that was pre-incubated with an anti-Cβ antibody (B). For each sensorgram, the nonspecific responses to empty sensor chips were subtracted. Representatives of two independent experiments with similar results are shown.

anti-Cβ antibody pre-coated plate. After washing, the OT-1 TCR-Fc was incubated with OVA-p/MHC tetramers to examine whether the OT-1 TCR-Fc protein bound to the OVA-p/MHC tetramer. The OT-1 TCR-Fc protein that bound to the plate coated with the anti-Cβ antibody bound the OVA-p/MHC tetramer (Fig. 1D). The control p/MHC tetramer did not bind to the OT-1 TCR-Fc protein (Fig. 1D). These results demonstrate that the OT-1 TCR-Fc protein immobilized with an anti-Cβ antibody bound to the OVA-p/MHC tetramer.

3.3. Improvement of the binding affinity of the OT-1 TCR-Fc protein

To investigate the effect of the anti-Cβ antibody on the OT-1 TCR-Fc protein, we performed surface plasmon resonance (SPR) assays using an OVA-p/MHC monomer-bound chip. The sensorgram of the OT-1 TCR-Fc protein with the OVA-p/MHC monomer showed very low binding affinity with a very fast dissociation rate (Fig. 2A). The binding affinity (*K*D) of the OT-1 TCR-Fc protein with the OVA-p/MHC monomer was estimated to be 1.1×10^{-5} M. The *K*D value of our results using purified α/β heterodimer was 1.1×10^{-5} M, which was almost comparable (1.7-fold lower) to that of Alam et al. study (6.5×10^{-6} M) [24]. In contrast, the binding affinity of the OT-1 TCR-Fc protein that had been pre-incubated with an anti-Cβ antibody was higher (2.2×10^{-6} M) than that of the OT-1 TCR-Fc protein alone (Fig. 2B). A control p/MHC monomer did not bind to the OT-1 TCR-Fc protein (data not shown). These results indicate that the binding affinity of the OT-1 TCR-Fc protein was increased by the anti-Cβ antibody.

4. Discussion

In this study, we generated an sTCR-Fc fusion protein that was composed of the TCR-V and TCR-C regions of the OT-1-TCR and the Ig Fc region (Supplementary Fig. 1) and showed that the Vα, Vβ, and Cβ domains of the fusion protein remained intact (Fig. 1). Using sandwich ELISAs, we showed that an OT-1 TCR-Fc protein immobilized by an anti-Cβ antibody effectively bound to an OVA-p/MHC tetramer. Using an SPR assay, we also demonstrated that the binding affinity of the OT-1 TCR-Fc to the OVA p/MHC monomer was markedly increased by 5-fold when the OT-1 TCR-Fc was crosslinked by an anti-Cβ antibody (Fig. 2).

Many investigators have constructed various sTCRs, such as heterodimers of the TCR α/β chains [7,8,17], two TCR variable domains joined into a single chain (scFV-TCRs) [9–12], or a TCR that was fused to a full-length Ig molecule [13–16]. The affinity (*K*D values) of sTCRs for the p/MHC is very low (with the range of $1–100 \times 10^{-6}$ M) compared to that of antibodies [1,18,19]. The low affinity of sTCRs is one of the major hurdles to their therapeutic and diagnostic application. Thus, several investigators have attempted to improve their binding affinity with two technologies. One such technology involves optimization of the CDR3 of the TCR V region by amino acid replacement [20–22], which significantly increased the affinity of TCRs by at least $\sim 10^3$-fold. The other technique uses TCR phage display technology [25]. This technology dramatically increased the affinity of TCRs by at least $\sim 10^6$-fold [25]. However, these technologies are difficult to perform in ordinary laboratories. In the present study, we demonstrated that the binding affinity of an sTCR-Fc is easily improved by the addition of an anti-Cβ antibody.

The OT-1 TCR-Fc protein itself is monovalent, and crosslinking the OT-1 TCR-Fc protein with an anti-Cβ antibody makes the OT-1 TCR-Fc protein bivalent, resulting in an increase in the functional binding capacity (avidity) of the OT-1 TCR-Fc protein, similar to the case of bivalent antibodies [3]. However, the present study showed that an anti-Cβ antibody enhanced the binding affinity of an sTCR-Fc fusion protein to an OVA-p/MHC by approximately 5-fold (Fig. 2). What is the mechanism of the increased affinity of the sTCR by binding to the anti-Cβ antibody?

We propose a stability model in which the anti-Cβ antibody stabilizes the Vα/Vβ domains (FV) of the TCR by binding to an appropriate region of the Cβ domain. In this respect, Wang et al. showed that an anti-Cβ antibody binds to the looped-out polypeptide of the Cβ domain between the Vβ and Cβ domains, perpendicular to the Vβ/Cβ protein [26]. It is conceivable that the binding of the anti-Cβ antibody to Vβ/Cβ protein could stabilize the bent position of the Vβ and Cβ domains, which in turn could stabilize the FV conformation of the sTCR. To investigate this possibility, we are now analyzing the effect of the anti-Cβ antibody on the relative position of the Vα and Vβ domains using fluorescence resonance energy transfer (FRET) analysis.

In conclusion, we have demonstrated the utility of an anti-Cβ antibody in improving the binding affinity of an sTCR-Fc protein. Our findings may facilitate the use of soluble TCRs as a diagnostic or therapeutic tool for the treatment of cancer or infectious diseases by improving the binding affinity of soluble TCRs.

Acknowledgments

We thank Sanae Hirota for technical assistance and Kaoru Hata for administrative work. This research was supported by Grants

from the Hokuriku Innovation Cluster for the Health Science Project of the Ministry of Education, Culture, Sports, and Science of Japan, the Toyama and Ishikawa Prefectures, and Grants-in-Aid from the Ministry of Education, Culture, Sports, and Science of Japan.

Appendix A. Supplementary data

Supplementary data associated with this article can be found, in the online version, at http://dx.doi.org/10.1016/j.bbrc.2012.04.134.

References

[1] M.M. Davis, J.J. Boniface, Z. Reich, D. Lyons, J. Hampl, B. Arden, Y. Chien, Ligand recognition by alpha beta T cell receptors, Annu. Rev. Immunol. 16 (1998) 523–544.
[2] K.C. Garcia, L. Teyton, I.A. Wilson, Structural basis of T cell recognition, Annu. Rev. Immunol. 17 (1999) 369–397.
[3] A.K. Abbas, A.H. Lichtman, Cellular and Molecular Immunology, fifth ed. (Updated edition)., Elsevier, Amsterdam, 2005.
[4] J.M. Boulter, B.K. Jakobsen, Stable, soluble, high-affinity, engineered T cell receptors: novel antibody-like proteins for specific targeting of peptide antigens, Clin. Exp. Immunol. 142 (2005) 454–460.
[5] P.E. Molloy, A.K. Sewell, B.K. Jakobsen, Soluble T cell receptors: novel immunotherapies, Curr. Opin. Pharmacol. 5 (2005) 438–443.
[6] S.A. Richman, D.M. Kranz, Display, engineering, and applications of antigen-specific T cell receptors, Biomol. Eng. 24 (2007) 361–373.
[7] H.C. Chang, Z. Bao, Y. Yao, A.G. Tse, E.C. Goyarts, M. Madsen, E. Kawasaki, P.P. Brauer, J.C. Sacchettini, S.G. Nathenson, et al., A general method for facilitating heterodimeric pairing between two proteins: application to expression of alpha and beta T-cell receptor extracellular segments, Proc. Natl. Acad. Sci. USA 91 (1994) 11408–11412.
[8] A. Golden, S.S. Khandekar, M.S. Osburne, E. Kawasaki, E.L. Reinherz, T.H. Grossman, High-level production of a secreted, heterodimeric alpha beta murine T-cell receptor in *Escherichia coli*, J. Immunol. Methods 206 (1997) 163–169.
[9] C. Gregoire, S.Y. Lin, G. Mazza, N. Rebai, I.F. Luescher, B. Malissen, Covalent assembly of a soluble T cell receptor–peptide-major histocompatibility class I complex, Proc. Natl. Acad. Sci. USA 93 (1996) 7184–7189.
[10] K.S. Gunnarsen, E. Lunde, P.E. Kristiansen, B. Bogen, I. Sandlie, G.A. Loset, Periplasmic expression of soluble single chain T cell receptors is rescued by the chaperone FkpA, BMC Biotechnol. 10 (2010) 8.
[11] J. Kappler, J. White, H. Kozono, J. Clements, P. Marrack, Binding of a soluble alpha beta T-cell receptor to superantigen/major histocompatibility complex ligands, Proc. Natl. Acad. Sci. USA 91 (1994) 8462–8466.
[12] D.F. Lake, M.L. Salgaller, P. van der Bruggen, R.M. Bernstein, J.J. Marchalonis, Construction and binding analysis of recombinant single-chain TCR derived from tumor-infiltrating lymphocytes and a cytotoxic T lymphocyte clone directed against MAGE-1, Int. Immunol. 11 (1999) 745–751.
[13] M.S. Lebowitz, S.M. O'Herrin, A.R. Hamad, T. Fahmy, D. Marguet, N.C. Barnes, D. Pardoll, J.G. Bieler, J.P. Schneck, Soluble, high-affinity dimers of T-cell receptors and class II major histocompatibility complexes: biochemical probes for analysis and modulation of immune responses, Cell Immunol. 192 (1999) 175–184.
[14] E. Lunde, G.A. Loset, B. Bogen, I. Sandlie, Stabilizing mutations increase secretion of functional soluble TCR-Ig fusion proteins, BMC Biotechnol. 10 (2010) 61.
[15] L.A. Mosquera, K.F. Card, S.A. Price-Schiavi, H.J. Belmont, B. Liu, J. Builes, X. Zhu, P.A. Chavaillaz, H.I. Lee, J.A. Jiao, J.L. Francis, A. Amirkhosravi, R.L. Wong, H.C. Wong, In vitro and in vivo characterization of a novel antibody-like single-chain TCR human IgG1 fusion protein, J. Immunol. 174 (2005) 4381–4388.
[16] S.M. O'Herrin, M.S. Lebowitz, J.G. Bieler, B.K. al-Ramadi, U. Utz, A.L. Bothwell, J.P. Schneck, Analysis of the expression of peptide-major histocompatibility complexes using high affinity soluble divalent T cell receptors, J. Exp. Med. 186 (1997) 1333–1345.
[17] B.E. Willcox, G.F. Gao, J.R. Wyer, C.A. O'Callaghan, J.M. Boulter, E.Y. Jones, P.A. van der Merwe, J.I. Bell, B.K. Jakobsen, Production of soluble alphabeta T-cell receptor heterodimers suitable for biophysical analysis of ligand binding, Protein Sci. 8 (1999) 2418–2423.
[18] S.M. Alam, G.M. Davies, C.M. Lin, T. Zal, W. Nasholds, S.C. Jameson, K.A. Hogquist, N.R. Gascoigne, P.J. Travers, Qualitative and quantitative differences in T cell receptor binding of agonist and antagonist ligands, Immunity 10 (1999) 227–237.
[19] J.D. Stone, A.S. Chervin, D.M. Kranz, T-cell receptor binding affinities and kinetics: impact on T-cell activity and specificity, Immunology 126 (2009) 165–176.
[20] B.J. Hare, D.F. Wyss, M.S. Osburne, P.S. Kern, E.L. Reinherz, G. Wagner, Structure, specificity and CDR mobility of a class II restricted single-chain T-cell receptor, Nat. Struct. Biol. 6 (1999) 574–581.
[21] P.D. Holler, P.O. Holman, E.V. Shusta, S. O'Herrin, K.D. Wittrup, D.M. Kranz, In vitro evolution of a T cell receptor with high affinity for peptide/MHC, Proc. Natl. Acad. Sci. USA 97 (2000) 5387–5392.
[22] K.S. Weber, D.L. Donermeyer, P.M. Allen, D.M. Kranz, Class II-restricted T cell receptor engineered in vitro for higher affinity retains peptide specificity and function, Proc. Natl. Acad. Sci. USA 102 (2005) 19033–19038.
[23] J.M. Kelly, S.J. Sterry, S. Cose, S.J. Turner, J. Fecondo, S. Rodda, P.J. Fink, F.R. Carbone, Identification of conserved T cell receptor CDR3 residues contacting known exposed peptide side chains from a major histocompatibility complex class I-bound determinant, Eur. J. Immunol. 23 (1993) 3318–3326.
[24] S.M. Alam, P.J. Travers, J.L. Wung, W. Nasholds, S. Redpath, S.C. Jameson, N.R. Gascoigne, T-cell-receptor affinity and thymocyte positive selection, Nature 381 (1996) 616–620.
[25] Y. Li, R. Moysey, P.E. Molloy, A.L. Vuidepot, T. Mahon, E. Baston, S. Dunn, N. Liddy, J. Jacob, B.K. Jakobsen, J.M. Boulter, Directed evolution of human T-cell receptors with picomolar affinities by phage display, Nat. Biotechnol. 23 (2005) 349–354.
[26] J. Wang, K. Lim, A. Smolyar, M. Teng, J. Liu, A.G. Tse, J. Liu, R.E. Hussey, Y. Chishti, C.T. Thomson, R.M. Sweet, S.G. Nathenson, H.C. Chang, J.C. Sacchettini, E.L. Reinherz, Atomic structure of an alphabeta T cell receptor (TCR) heterodimer in complex with an anti-TCR fab fragment derived from a mitogenic antibody, EMBO J. 17 (1998) 10–26.

Citation: Molecular Therapy–Nucleic Acids (2012) 1, e63; doi:10.1038/mtna.2012.52

www.nature.com/mtna

A Promising Vector for TCR Gene Therapy: Differential Effect of siRNA, 2A Peptide, and Disulfide Bond on the Introduced TCR Expression

Sachiko Okamoto[1], Yasunori Amaishi[1], Yumi Goto[1], Hiroaki Ikeda[2], Hiroshi Fujiwara[3], Kiyotaka Kuzushima[4], Masaki Yasukawa[3], Hiroshi Shiku[2] and Junichi Mineno[1]

Adoptive immunotherapy using TCR gene-modified T-lymphocytes is an attractive strategy for targeting malignancies. However, TCR mispairings between endogenous and introduced TCR chains are a major concern, as they may induce mixed TCRs with unknown specificities and may reduce the expression of therapeutic TCRs. To overcome these problems, we have recently established a novel retroviral siTCR vector encoding small-interfering RNAs (siRNAs) to knockdown endogenous TCR genes for the efficient expression of therapeutic TCRs. In this study, to improve the efficacy of siTCR vectors, we developed 2A peptide-based siTCR vectors that could increase the expression levels of transduced TCRs compared with internal promoter-based siTCR vectors. We also evaluated the efficacy of an siTCR strategy and the addition of a new interchain disulfide bond created by cysteine modification. We found that the effect of the cysteine modification depended on TCR variations, while the siTCR strategy improved the expression of all TCRs tested. Furthermore, the combined effect of the siTCR and cysteine modification strategies was highly significant for certain TCRs. Therefore, our novel siTCR technology, in isolation or in combination with another strategy, may open the door to effective immunotherapy for cancer patients.
Molecular Therapy–Nucleic Acids (2012) **1**, e63; doi:10.1038/mtna.2012.52; published online 18 December 2012
Subject Category: Gene Vectors

Introduction

The adoptive transfer of tumor-reactive T cells has been shown to mediate the regression of tumors.[1] A limitation of this treatment is the difficulty of isolating and expanding pre-existing, highly tumor-reactive lymphocytes from patients. Adoptive immunotherapy using TCR gene-modified T cells is a promising strategy for producing tumor antigen-specific T cells by converting the abundant numbers of existing primary lymphocytes. The feasibility of TCR gene therapy was demonstrated in a recent report on clinical trials with TCR gene-transferred T cells. However, further technical improvements may be required to achieve excellent clinical responses and reduce potential dangers.[2–9]

The inefficient surface expression of transduced TCRs has been reported to directly affect the efficacy of TCR gene therapy. The existence of endogenous TCRs is one of the major reasons for inefficient expression of the introduced TCRs. Given that the surface expression of TCRs requires assembly with CD3 subunits, which are limiting, endogenous and exogenous TCRs may be competing for CD3 subunits.[10] Moreover, exogenous TCRs can also join with endogenous TCRs, thus decreasing the surface expression of exogenous TCR$\alpha\beta$ chains. In addition to the decrease in introduced TCR expression, mixed TCR dimers with unknown specificities generated by TCR mispairing can also cause autoimmunity, thus adversely affecting the safety of TCR gene therapy.[11,12] Another safety issue in TCR gene therapy is the copy number of the integrated vector. Although the expression level of the transgenes can be enhanced by increasing the vector copy number,[13] a low copy number is necessary for reducing the risk of promoting the proto-oncogene activation, tumor-suppressor gene activation, and chromosomal instability caused by insertional mutagenesis.[14–16] Thus, a strategy for achieving a high expression of introduced TCRs without TCR mispairing and with relatively low vector copy numbers would be ideal.

A number of approaches have been reported to minimize TCR mispairing, including replacing the human TCR constant region sequences with murine sequences, the introduction of cysteine residues to mediate the interchain disulphide bridge, and the fusion of the TCR chains to human CD3ζ.[17–22] We recently developed a novel system that can highly express therapeutic TCRs while suppressing the expression of endogenous TCRs by using siTCR retroviral vector encoding antigen-specific TCRs and small-interfering RNAs (siRNAs) against endogenous TCRs. The T cells transduced with siTCR retroviral vector encoding HLA-A*2402-restricted MAGE-A4- or WT1-specific TCRs showed an enhanced expression of introduced TCRs and an enhanced biological function at relatively low vector numbers *in vitro* and in a mouse model.[23,24]

To improve the efficacy of the siTCR vector system, more efficient expression of transduced TCRs and siRNAs is essential. Several strategies have been employed to construct bicistronic vectors, including an internal promoter, an internal ribosomal entry site,[4] and a self-cleaving 2A peptide. Recently,

[1]Center for Cell and Gene Therapy, Takara Bio Inc., Shiga, Japan; [2]Department of Immuno-Gene Therapy, Mie University Graduate School of Medicine, Mie, Japan; [3]Department of Bioregulatory Medicine, Ehime University Graduate School of Medicine, Ehime, Japan; [4]Division of Immunology, Aichi Cancer Center Research Institute, Aichi, Japan. Correspondence: Junichi Mineno, Center for Cell and Gene therapy, Takara Bio Inc., SETA 3-4-1, Otsu, Shiga, 520-2193, Japan. E-mail: minenoj@takara-bio.co.jp
Keywords: mixed TCR; retroviral vector; siRNA; TCR gene therapy
Received 14 September 2012; accepted 9 October 2012; advance online publication 18 December 2012. doi:10.1038/mtna.2012.52

2A peptides have been widely adopted for TCR gene therapy because of their comparative stoichiometric expression of both chains.[2,3,6,25,26] In this study, we attempted to develop the ideal 2A peptide-based siTCR retroviral vector that can achieve a high expression of therapeutic TCRs without a mixed TCR dimer formation at limited vector copy numbers, thus providing an efficient and safe therapy.

Results

Retroviral vector using 2A peptides facilitates the expression of transgenes but is not sufficient for preventing TCR mispairing

For our first-generation siTCR retroviral vector, we used an internal promoter to express two TCR genes.[23] To explore more efficient siTCR retroviral vectors, an increase in the TCR expression per vector copy would be desirable. We therefore evaluated the expression level of TCR genes by bicistronic vectors using the 2A peptide and an internal promoter. We compared retroviral vectors encoding MAGE-A4–specific TCRs using pMS[23] or pMS3 retroviral vector backbones. pMS vector is a derivative of pMT which is a minimum-sized murine leukemia virus-based vector that contains no viral-coding sequences. The 3′-long terminal repeat (LTR) of pMT was replaced with the murine stem cell virus LTR to generate pMS vector. pMS3 vector was constructed by inserting the portion of intron and splice acceptor region from the human EF1-α from pMIN5 vector into pMS vector, which can increase the transgene expression *via* RNA splicing,[27–30] and the surface expression levels of transduced TCR were higher in the peripheral blood mononuclear cells (PBMCs) transduced with the MS3 vector compared with the MS vector (**Supplementary Figure S1**). To accurately compare the efficacy of the retroviral vectors, we evaluated it based on the proviral copy number in transduced PBMCs to normalize the titer of each vector. We therefore adopted the MS3 backbone for the WT1- and human telomerase reverse transcriptase (hTERT)-specific TCRs (**Figure 1a**). The RNA expression levels of all TCRs tested in this study were higher in the PBMCs transduced with vectors using the T2A peptide than those transduced with internal promoter-typed vectors (data not shown). The expression of WT1-specific TCRs in the PBMCs transduced with MS3-a2Ab was almost twice that of those transduced with MS3-aPb at the same proviral copy number (**Figure 1a,b**), and MS3-a2Ab was able to yield higher numbers of tetramer-positive cells at relatively lower proviral copy numbers than MS3-aPb and MS3-aPb-siTCR were (**Figure 1d**). Although the expression levels of TCR Vβ2 chain which is utilized by the hTERT-specific TCR were twice as high in the PBMCs transduced with the MS3-a2Ab vector as in those transduced with MS3-aPb at equivalent proviral copy numbers, the increased TCR expression using the T2A peptide by itself could not improve the hTERT-specific TCRαβ heterodimer expression on the cell surface in the MS3-a2Ab–transduced cells. The MS3-aPb-siTCR vector was able to achieve a higher expression of

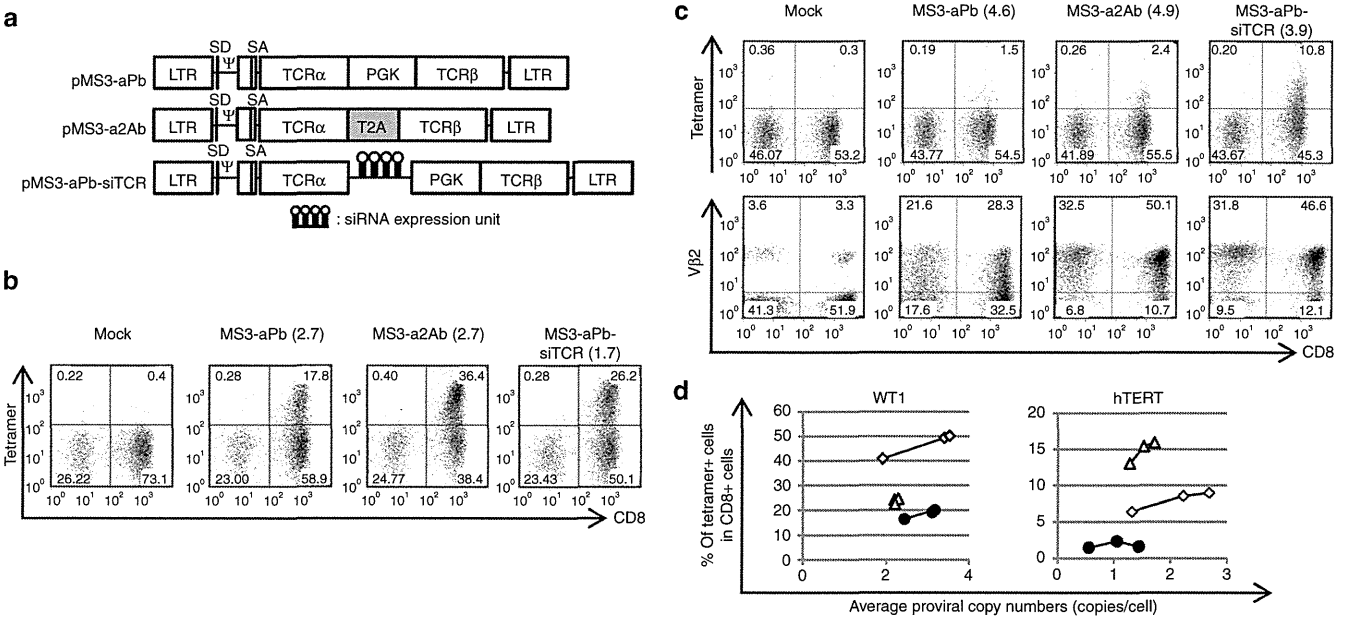

Figure 1 The 2A peptide can increase the expression of each TCR chain, but it is not sufficient for efficient surface expression. (**a**) Schema of the retroviral vectors used to transduce the PBMCs. pMS3-aPb and pMS3-aPb-siTCR are internal promoter-based vectors, while pMS3-a2Ab is a vector using the T2A peptide. (**b–d**) PBMCs from more than three different donors were transduced with serially diluted retroviral vectors and used for tetramer staining and proviral copy number analysis, and anti-TCR Vβ2 Ab staining was performed for hTERT-specific TCRs. Representative flow cytometry analysis of PBMCs transduced with (**b**) WT1- and (**c**) hTERT-specific TCR expression vectors, with proviral copy numbers indicated in parentheses. (**d**) The percentages of tetramer-positive cells among the CD8+ cells in MS3-aPb (closed circles), MS3-a2Ab (open diamonds), and MS3-aPb-siTCR- (open triangles) transduced cells are plotted according to the copy number using the distinct donors used in **b** and **c**. ψ, packaging signal; hTERT, human telomerase reverse transcriptase; LTR, long terminal repeat of M-MLV (5′LTR) and MSCV (3′LTR); MLV, murine leukemia virus; MSCV, murine stem cell virus; PBMC, peripheral blood mononuclear cell; PGK, phosphoglycerate kinase promoter; SA, splice acceptor; SD, splice donor; siRNA, small-interfering RNA; T2A, -SGSG-linker peptide+T2A peptide; TCRα, codon-optimized TCRα chain; TCRβ, codon-optimized TCRβ chain.

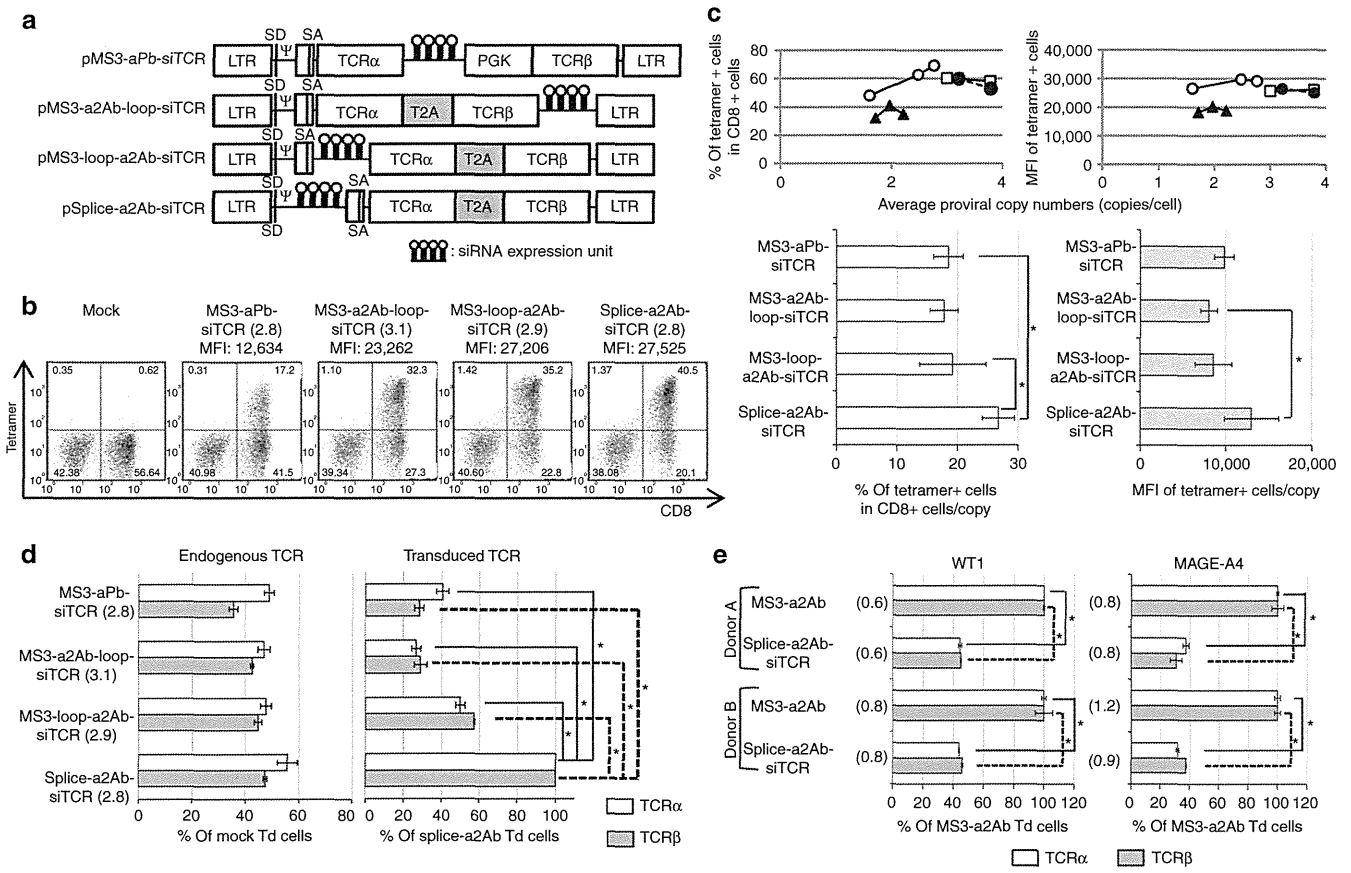

Figure 2 2A peptide-typed siTCR retroviral vectors can increase the surface expression of TCR. (**a**) Schema of retroviral vectors used to transduce the PBMCs. pMS3-aPb-siTCR, pMS3-a2Ab-loop-siTCR, pMS3-loop-a2Ab-siTCR, and pSplice-a2Ab-siTCR were constructed to express WT1-specific TCRs. (**b**,**c**) PBMCs from more than three different donors were transduced with serially diluted retroviral vectors and used for tetramer staining and proviral copy number analysis. (**b**) Representative flow cytometry analysis of the PBMCs transduced with WT1-expressing siTCR vectors, with equivalent proviral copy numbers indicated in parentheses. The MFIs of the tetramer are also indicated. (**c**) The percentages of tetramer-positive cells among the CD8+ cells in the MS3-aPb-siTCR- (closed triangles), MS3-loop-a2Ab-siTCR- (closed circles), MS3-a2Ab-loop-siTCR- (open squares), and Splice-a2Ab-siTCR- (open circles) transduced PBMCs are plotted according to the copy number using the distinct donors used in **b**. The percentages of tetramer-positive cells per proviral copy and the MFI of tetramer per proviral copy were calculated and evaluated by Student's *t*-test. Data are mean ± SD. $^*P < 0.05$. (**d**) Bulk PBMCs transduced with siTCR retroviral vectors with similar copy numbers shown in **b** were collected, and endogenous and transduced codon-optimized TCRα and β RNAs expression were quantified. The expression level of endogenous TCRs was calculated as the percentage of mock-transduced PBMCs, and transduced codon-optimized TCRs were calculated as the percentage of the PBMCs transduced with Splice-a2Ab-siTCR. These experiments were conducted with PBMCs from more than three donors with similar results. Data are mean ± SD. $^*P < 0.05$. (**e**) The tetramer-positive cells were collected from MS3-a2Ab- or Splice-a2Ab-siTCR–transduced bulk PBMCs with similar copy numbers shown in parentheses and endogenous TCRα and β RNAs were quantified. The expression level of endogenous TCRs was calculated as the percentage of MS3-a2Ab–transduced PBMCs. Data are mean ± SD. $^*P < 0.05$. ψ, packaging signal; LTR, long terminal repeat of M-MLV (5′LTR) and MSCV (3′LTR); MFI, mean fluorescence intensity; MLV, murine leukemia virus; MSCV, murine stem cell virus; PBMC, peripheral blood mononuclear cell; PGK, phosphoglycerate kinase promoter; SA, splice acceptor; SD, splice donor; siRNA, small-interfering RNA; T2A, -SGSG-linker peptide+T2A peptide; TCRα, codon-optimized TCRα chain; TCRβ, codon-optimized TCRβ chain; Td, transduced.

therapeutic TCRs than the MS3-aPb and MS3-a2Ab vectors were (Figure 1c,d). Increasing the expression level of the transduced TCRs using the 2A peptide was effective but not sufficient for efficient surface expression of the transduced TCRs without TCR mispairing.

Development of efficient siTCR retroviral vectors using the 2A peptide

In an attempt to develop more efficient siTCR retroviral vectors for TCR gene therapy, we constructed several retroviral vectors encoding WT1-specific TCRs using the T2A peptide and siRNAs to knockdown endogenous TCRs (Figure 2a). Compared with the first-generation siTCR retroviral vector (MS3-aPb-siTCR; PM11-w in previous report),[23] all siTCR vectors using the T2A peptide yielded a higher surface expression of WT1-specific TCRs at equivalent proviral copy numbers (Figure 2b) and showed a higher percentage and expression level at lower proviral copy numbers, especially in Splice-a2Ab-siTCR–transduced T cells, when compared with the internal promoter-based siTCR vector MS3-aPb-siTCR (Figure 2b,c). To evaluate the knockdown efficiencies of endogenous TCRs and the expression level of ectopic TCR RNA, endogenous and transduced codon-optimized TCR RNA expression levels were quantified in bulk PBMCs

transduced with each retroviral vector, with the comparable proviral copy numbers shown in **Figure 2b**. All siTCR vectors were able to reduce the expression of endogenous TCRs at 40–50% of the mock-transduced PBMCs, even the bulk-transduced PBMCs containing nontransduced cells were used for analysis (**Figure 2d**, left). However, the RNA expression levels of the ectopic TCRs in the PBMCs transduced with MS3-aPb-siTCR, MS3-loop-a2Ab-siTCR, and MS3-a2Ab-loop-siTCR were lower than those in the Splice-a2Ab-siTCR vector (**Figure 2d**, right). The Splice-a2Ab-siTCR vector, one of the newly constructed siTCR vectors, had a siRNA expression unit inserted between the splice donor and the intron and splice acceptor region from the human EF1-α and expressed siRNAs by RNA splicing without lowering the RNA expression of ectopic TCRs. This vector was able to achieve the highest surface expression of WT1-specific TCRs, in terms of percentage and mean fluorescence intensity (MFI) at relatively low proviral copy numbers (**Figure 2c**). To elucidate the knockdown efficiency of endogenous TCRs, we have compared the expression level of endogenous TCRs in tetramer-positive cells separated from bulk-transduced PBMCs with WT1- or MAGE-A4–specific TCR-expressing MS3-a2Ab or Splice-a2Ab-siTCR vectors with the comparable proviral copy numbers shown in **Figure 2e**. Even we have analyzed the PBMCs with very low proviral copy number, the expression of endogenous TCRα and β in the Splice-a2Ab–transduced T cells were reduced at 30–45% of the MS3-a2Ab–transduced T cells (**Figure 2e**). We then tested whether the order of the TCRα and β genes linked by the 2A peptide could affect the surface expression of ectopic TCRs. As shown in **Figure 3a**, pMS3-a2Ab, pMS3-b2Aa, pSplice-a2Ab-siTCR, and pSplice-b2Aa-siTCR retroviral vectors were constructed to express WT1-, MAGE-A4-, and hTERT-specific TCRs. At comparable vector copy numbers, the PBMCs transduced with MS3-b2Aa and Splice-b2Aa-siTCR showed a higher percentage and MFI than did the cells transduced with MS3-a2Ab and Splice-a2Ab-siTCR, respectively, for all TCRs tested (**Figure 3b,c**). The Splice-a2Ab-siTCR and Splice-b2Aa-siTCR retroviral vectors achieved more efficient expression of ectopic TCRs than did the MS3-a2Ab and MS3-b2Aa vectors, respectively,

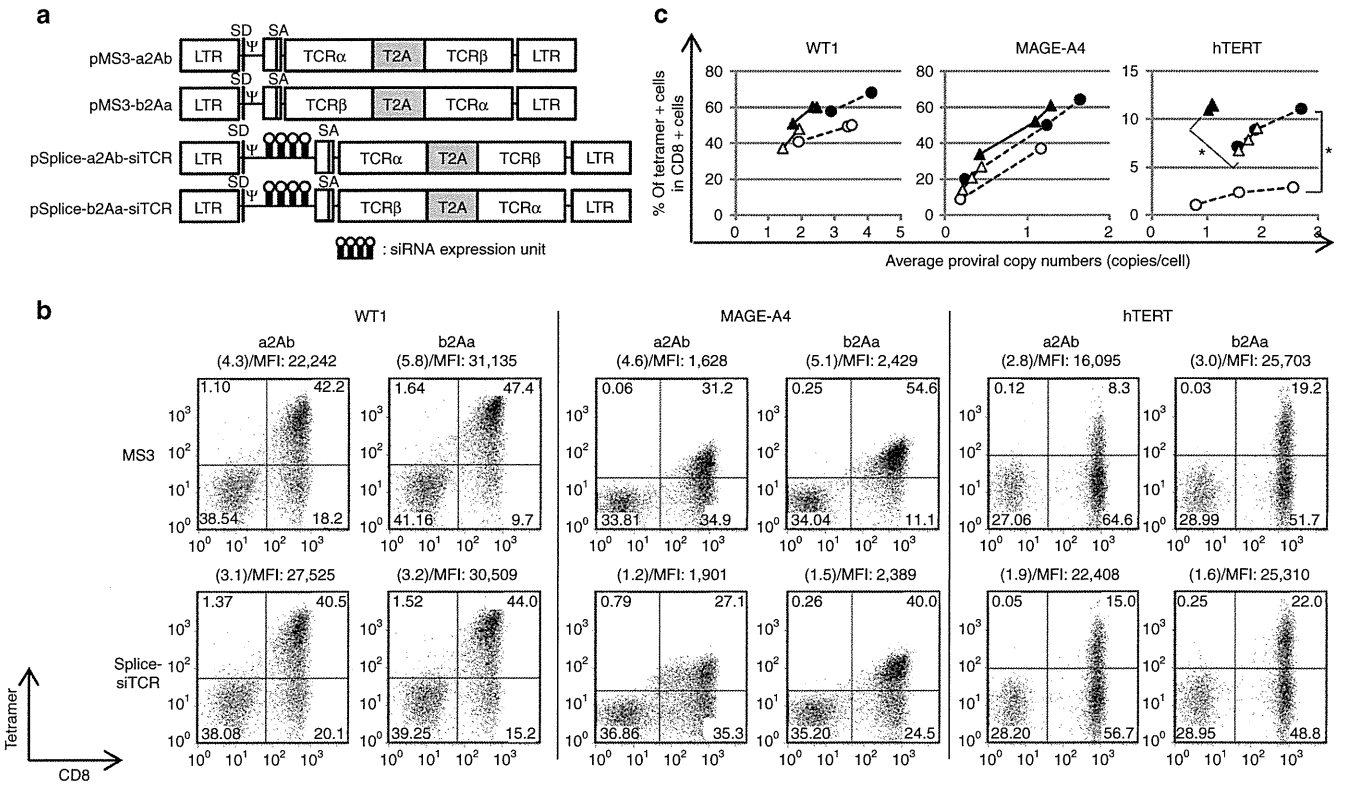

Figure 3 The order of TCRα and β genes connected by the T2A peptide affects TCR cell surface expression. (**a**) Schema of the retroviral vectors used to transduce the PBMCs. The pMS3-a2Ab, pMS3-b2Aa, pSplice-a2Ab-siTCR, and pSplice-b2Aa-siTCR were constructed to express WT1-, MAGE-A4-, hTERT-specific TCRs. (**b**,**c**) PBMCs from more than three different donors were transduced with serially diluted retroviral vectors and used for tetramer staining and proviral copy number analysis. (**b**) Representative flow cytometry analysis of PBMCs transduced with WT1-, MAGE-A4-, and hTERT-specific TCR-expressing vectors, with comparable proviral copy numbers indicated in parentheses. The MFIs of the tetramer are also indicated. (**c**) The percentages of tetramer-positive cells among the CD8+ cells in MS3-a2Ab- (open circles), MS3-b2Aa- (closed circles), Splice-a2Ab-siTCR- (open triangles), and Splice-b2Aa-siTCR- (closed triangles) transduced PBMCs are plotted according to the copy number. The percentages of tetramer-positive cells per proviral copy were calculated and evaluated by Student's *t*-test. **P* < 0.05. The PBMCs used in **b** and **c** are from separate donors. ψ, packaging signal; hTERT, human telomerase reverse transcriptase; LTR, long terminal repeat of M-MLV (5′LTR) and MSCV (3′LTR); MFI, mean fluorescence intensity; MLV, murine leukemia virus; MSCV, murine stem cell virus; PBMC, peripheral blood mononuclear cell; PGK, phosphoglycerate kinase promoter; SA, splice acceptor; SD, splice donor; siRNA, small-interfering RNA; T2A, -SGSG-linker peptide+T2A peptide; TCRα, codon-optimized TCRα chain; TCRβ, codon-optimized TCRβ chain.

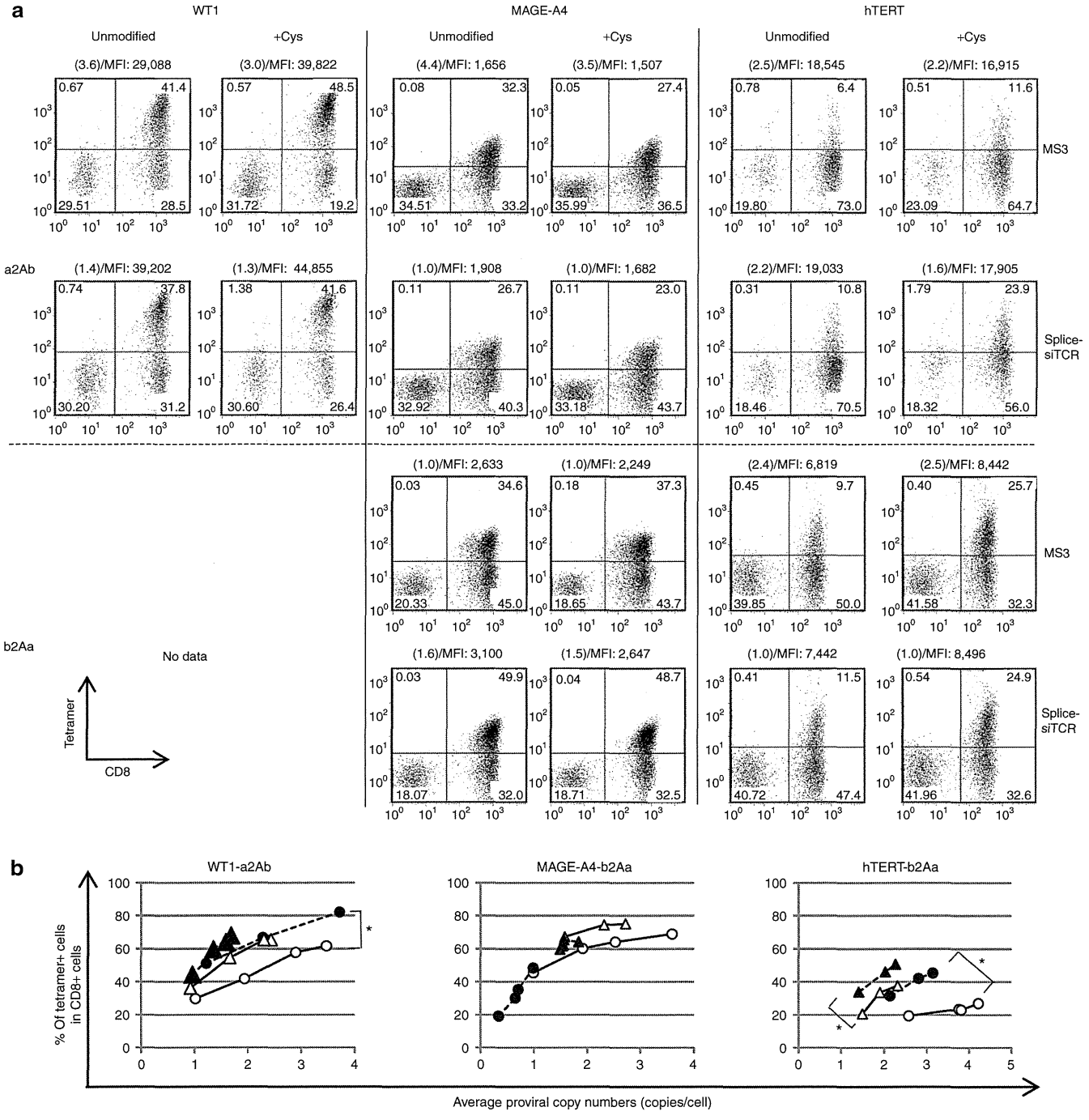

Figure 4 Cysteine modification is effective, but it is not sufficient for efficient expression. PBMCs from more than three different donors were transduced with serially diluted unmodified and cysteine-modified retroviral vectors (MS3-a2Ab and Splice-a2Ab-siTCR, expressing WT1-, MAGE-A4-, and hTERT-specific TCRs; and MS3-b2Aa and Splice-b2Aa-siTCR, expressing MAGE-A4- and hTERT-specific TCRs) and used for tetramer staining and proviral copy number analysis. (**a**) Representative flow cytometry analysis of the PBMCs transduced with WT1-, MAGE-A4-, and hTERT-specific TCR-expressing vectors, with equivalent proviral copy numbers indicated in parentheses. The MFIs of the tetramer are also indicated. (**b**) The percentage of tetramer-positive cells among CD8+ cells in unmodified (open circles) and cysteine-modified (closed circles) MS3-a2Ab encoding WT1-specific TCRs and MS3-b2Aa encoding MAGE-A4- and hTERT-specific TCRs, and unmodified (open triangles) and cysteine-modified (closed triangles) Splice-a2Ab-siTCR (for WT1) and Splice-b2Aa-siTCR (for MAGE-A4 and hTERT) cells are plotted according to the copy number. The percentages of tetramer-positive cells per proviral copy were caluculated and evaluated by Student's *t*-test. $^*P < 0.05$. The PBMCs used in **a** and **b** are from separate donors. hTERT, human telomerase reverse transcriptase; MFI, mean fluorescence intensity; PBMC, peripheral blood mononuclear cell.

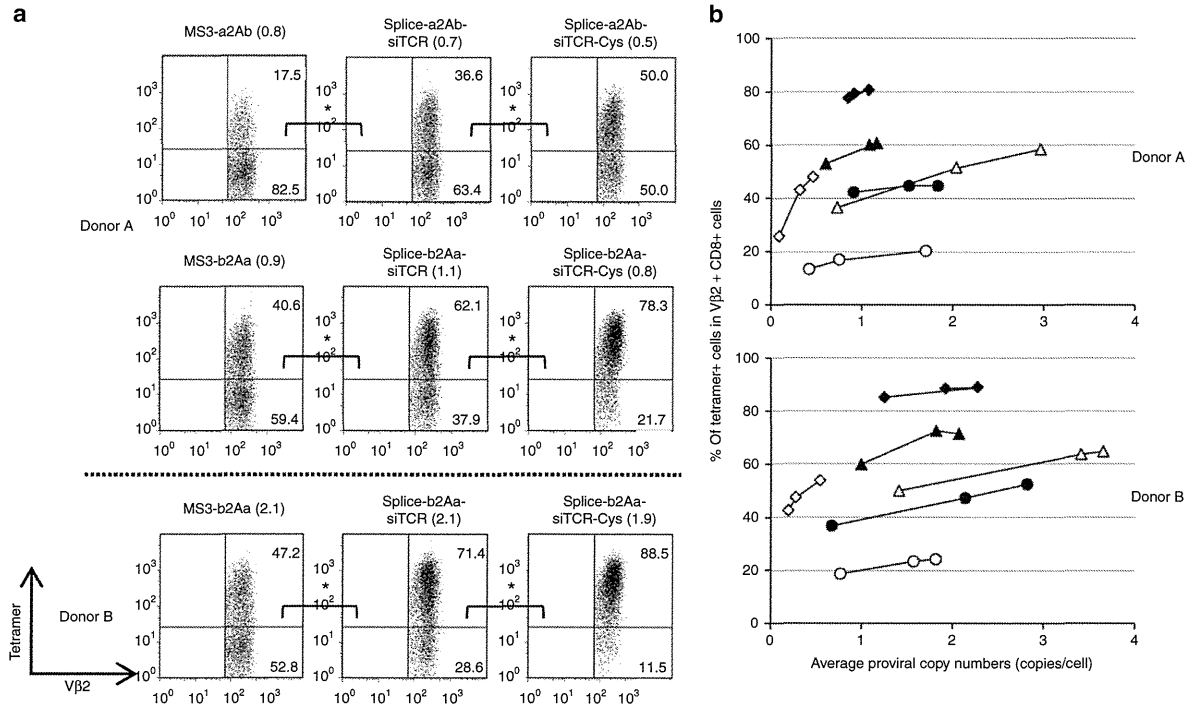

Figure 5 siTCR technology and the combination of siTCR and cysteine modification reduced the mixed TCRs and facilitated the expression of desired TCRs. PBMCs from two different donors were transduced with serially diluted unmodified and cysteine-modified retroviral vectors, MS3-a2Ab, Splice-a2Ab-siTCR, cysteine-modified Splice-a2Ab-siTCR-Cys, MS3-b2Aa, Splice-b2Aa-siTCR, and cysteine-modified Splice-b2Aa-siTCR-Cys retroviral vectors expressing hTERT-specific TCRs. The proviral copy number analysis and triple-staining with hTERT-tetramer, anti-CD8 Ab, and anti-Vβ2 Ab were performed. (**a**) Representative flow cytometry analysis of the PBMCs transduced with hTERT-specific TCR-expressing vectors, with equivalent proviral copy numbers indicated in parentheses. The staining were repeated three times and evaluated by Student's *t*-test. $^*P < 0.05$. (**b**) The percentage of tetramer-positive cells among CD8+ and Vβ2+cells in MS3-a2Ab (open circles), unmodified (open triangles)- and cysteine-modified (open diamonds)- Splice-a2Ab-siTCR, MS3-b2Aa (closed circles), unmodified (closed triangles)- and cysteine-modified (closed diamonds)- Splice-b2Aa-siTCR are plotted according to the copy number. hTERT, human telomerase reverse transcriptase; PBMC, peripheral blood mononuclear cell.

for all TCRs tested, thus demonstrating the usability of the siTCR system for efficient TCR expression (Figure 3c). Therefore, the Splice-b2Aa-siTCR retroviral vector was the most suitable vector for achieving a higher surface expression of ectopic TCRs.

Cysteine modification improved the expression of WT1-, hTERT-specific TCRs but not the expression of MAGE-A4–specific TCRs, while the siTCR vector exerted global effects

To compare the efficacy of siTCR technology with other strategies for reducing TCR mispairing, we evaluated the efficacy of adding a new interchain disulfide bond created by cysteine modifications.[17,21] Using mutagenesis, we modified residue 48 of the Cα region from Thr to Cys and residue 57 of the Cβ region from Ser to Cys in the pMS3-a2Ab, pMS3-b2Aa, pSplice-a2Ab-siTCR, and pSplice-b2Aa-siTCR to construct the retroviral vectors encoding the WT1-, MAGE-A4-, and hTERT-specific TCRs containing additional cysteine residues. We then used the vectors to transduce the PBMCs. We performed tetramer staining and proviral copy number analysis and compared the PBMCs with equivalent proviral copy numbers and determined that the additional disulfide bond improved the pairing of the transduced TCRαβ chains and resulted in a more efficient expression of the WT1- and hTERT-specific TCRs in comparison with the unmodified TCRs transduced with both MS3 and Splice-siTCR vector constructs. In comparison, cysteine modification of the MAGE-A4–specific TCRs did not improve the cell surface expression of the introduced TCRs (Figure 4a,b). On the contrary, the siTCR vectors improved the expression of all TCRs tested in this study (Figures 3 and 4) and the expression of more than five other TCRs (data not shown) compared with the control vectors without siRNA expression. Furthermore, the combination of cysteine modification and siTCR technology yielded the most efficient expression of WT1- and hTERT-specific TCRs, showing the importance of eliminating endogenous TCRs for the efficient expression of introduced TCRs and not just for enhancing correct pairing between the transduced TCRαβ chains (Figure 4).

siTCR technology reduced the formation of mixed TCRs and improved the reactivity

To clearly demonstrate the reduction in TCR mispairing that results from siTCR technology combined with cysteine modification, we selected hTERT-specific TCRs that tend to be mispaired with endogenous TCRs more often than with MAGE-A4– or WT1-specific TCRs. Gene-modified PBMCs with hTERT-specific TCR-expressing vectors were triple-stained with CD8 Ab, Vβ2 Ab, and hTERT tetramers. When

we compared transduced T cells with equivalent proviral copy numbers, almost 83, 63, and 50% of the Vβ2-positive cells among CD8-positive cells were tetramer-negative in the MS3-a2Ab-, Splice-a2Ab-siTCR, and Splice-a2Ab-siTCR-Cys–transduced T cells, respectively. Correspondingly, the siTCR technology reduced the proportion of tetramer-negative cells from ~59 to 38% in the MS3-b2Aa and Splice-b2Aa-siTCR–transduced T cells, and the combination with cysteine modification showed a further reduction of mispairing to ~22% in the Splice-b2Aa-siTCR-Cys–transduced T cells. When we analyzed the transduced T cells from other donor with higher proviral copy numbers, almost 53, 29, and 12% of the Vβ2-positive cells among CD8-positive cells were tetramer-negative in the MS3-b2Aa-, Splice-b2Aa-siTCR, and Splice-b2Aa-siTCR-Cys–transduced T cells, respectively (**Figure 5a,b**). These results demonstrated that the siTCR technology reduced TCR mispairing to some extent and that the combination of siTCR with cysteine modification showed superior effects in reducing the formation of mixed TCRs. We then performed intracellular cytokine staining using MAGE-A4– and WT1-specific TCR gene-modified T cells stimulated with MAGE-A4 or WT1 peptide-pulsed T2A24 cells. The percentage of interferon-γ (IFNγ) or tumor necrosis factor-α (TNFα)-positive cells and the MFI of the PE-IFNγ or APC-TNFα were plotted according to the proviral copy numbers (**Figure 6a,b**). In the case of MAGE-A4–specific TCR-transduced T cells, MS3-b2Aa showed a equivalent proportion of PE-IFNγ- and TNFα-secreting cells to that of Splice-b2Aa-siTCR and Splice-b2Aa-siTCR-Cys, the Splice-b2Aa-siTCR and Splice-b2Aa-siTCR-Cys–transduced T cells showed a higher MFI of APC-TNFα than did MS3-b2Aa, which was statistically significant (**Figure 6a**). Similar results were obtained with WT1-specific TCR gene-modified T cells, although the proportion of IFNγ-secreted cells was comparable, the significant difference was observed in the MFI of the PE-IFNγ of the Splice-a2Ab-siTCR-Cys–transduced T cells compared with that of MS3-a2Ab. Although the difference was not as significant, if we focused on the T cells with higher proviral copy number, Splice-a2Ab-siTCR and Splice-a2Ab-siTCR-Cys–transduced T cells showed higher amounts of APC-TNFα than MS3-a2Ab did, demonstrating the superiority of TCR cells modified by siTCR vectors in terms of biological activity (**Figure 6b**).

The stability of ectopic TCR expression in siTCR-transduced T cells and siTCR-retrovirus producer cell lines

To confirm the long-term expression of introduced TCRs, the bulk PBMCs transduced with WT1-, MAGE-A4–, hTERT-specific TCR-expressing Splice-b2Aa-siTCR vectors were cultured *in vitro* through day 35. The percentage of tetramer-positive cells per proviral copy number was sustained through day 35, showing the stable expression of ectopic TCRs for more than 1 month (**Figure 7a**). We have also evaluated the functional stability of the producer cells using the cloned PG13 cells transduced with Splice-b2Aa-siTCR vectors expressing WT1-specific TCR. The two cloned producer cell lines were passaged 10 times, the cells at 5 and 10 times passage were used to produce GaLV-pseudotyped retroviral vectors and proviral genome stability assay. The viruses at passage 10 showed higher percentage of tetramer-positive cells than the viruses at passage 5 with donor A, however, the opposite data were obtained with donor B, indicating the retroviruses at passage 10 sustained the functional activity (**Figure 7b**). Furthermore, the proviral genome of the Splice-b2Aa-siTCR retroviral vector in cloned

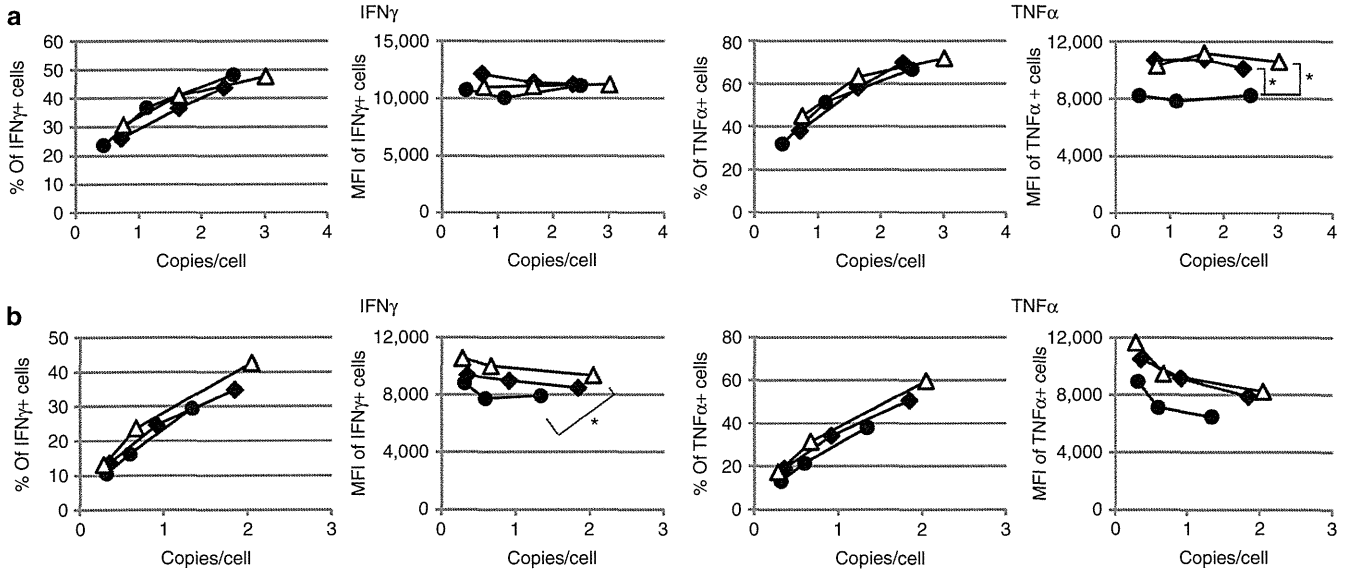

Figure 6 Increased cytokine secretion by TCR gene-modified T cells by siTCR vectors. The PBMCs were transduced with serially diluted (**a**) MAGE-A4–specific TCR-expressing retroviral vectors, MS3-b2Aa (closed circles), Splice-b2Aa-siTCR (closed diamonds), and cysteine-modified Splice-b2Aa-siTCR-Cys (open triangles), and (**b**) WT1-specific TCR-expressing retroviral vectors, MS3-a2Ab (closed circles), Splice-a2Ab-siTCR (closed diamonds), and cysteine-modified Splice-a2Ab-siTCR-Cys (open triangles), and used for proviral copy number analysis. Intracellular cytokine staining was performed using stimulated TCR gene-modified T cells with MAGE-A4$_{143\text{-}151}$ or WT1$_{235\text{-}243}$ peptide-pulsed T2A24 cells. The percentages of IFNγ- or TNFα-positive cells and the MFI of PE-IFNγ or APC-TNFα among CD8+ cells in (**a**) MAGE-A4- and (**b**) WT1-TCR–transduced cells are plotted according to the copy number. The MFI of PE-IFNγ and APC-TNFα were evaluated by Student's *t*-test. $^*P < 0.05$. IFN, interferon; MFI, mean fluorescence intensity; PBMC, peripheral blood mononuclear cell; TNF, tumor necrosis factor.

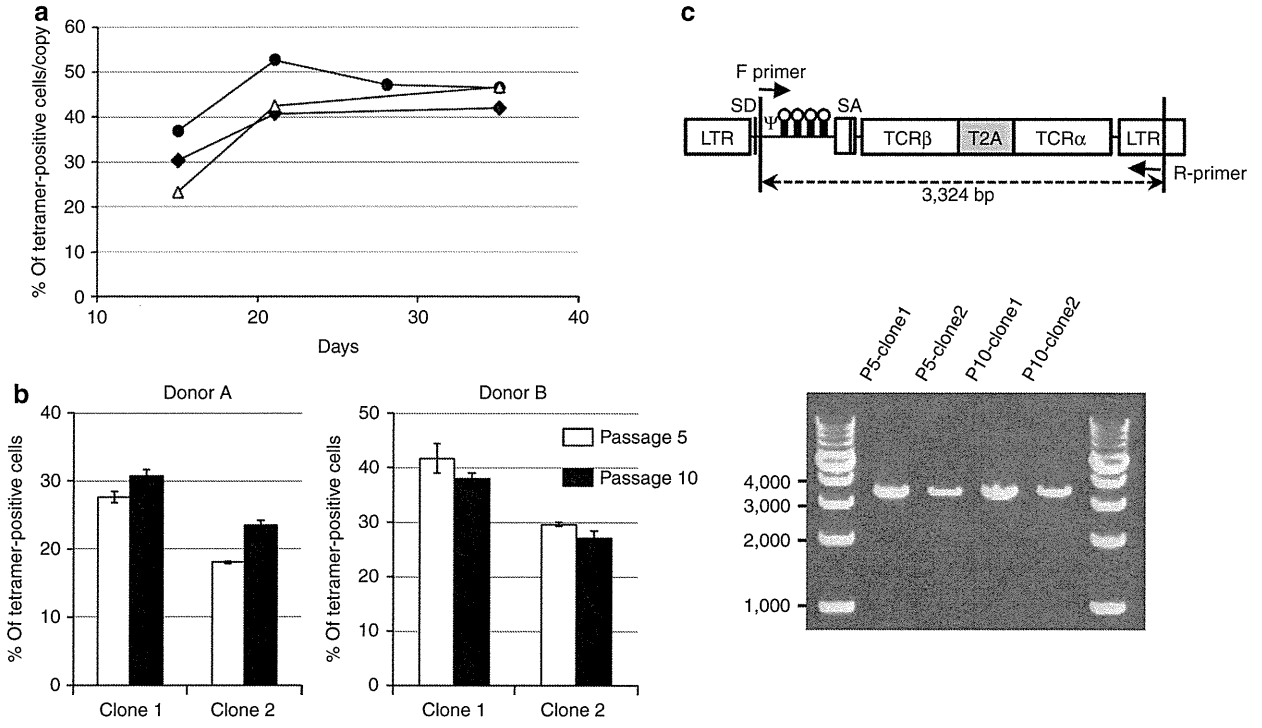

Figure 7 Stability of TCR expression in siTCR-transduced T cells and producer cell lines for siTCR vectors. (**a**) PBMCs were transduced with Splice-b2Aa-siTCR, expressing WT1 (open triangles)-, MAGE-A4 (closed circles)-, and hTERT (closed diamonds)-specific TCRs and used for tetramer staining and proviral copy number analysis on days 15, 21, 28 (only for MAGE-A4), and 35. The percentages of tetramer-positive cells per proviral copy were plotted. (**b**) The WT1-expressing-Splice-b2Aa-siTCR retroviruses obtained from two different cloned PG13 producer cell lines at passage number 5 and 10 were used to transduce PBMCs, and tetramer staining were performed. Data are mean ± SD of three different transduced PBMCs. (**c**) The genomic DNA from WT1-Splice-b2Aa-siTCR-PG13 producer cells lines were amplified by PCR. ψ, packaging signal; LTR, long terminal repeat; PBMC, peripheral blood mononuclear cell; SA, splice acceptor; SD, splice donor; siRNA, small-interfering RNA; T2A, -SGSG-linker peptide+T2A peptide; TCRα, codon-optimized TCRα chain; TCRβ, codon-optimized TCRβ chain.

PG13 producer cell lines were stable at passage 10, showing the stability of producer cell lines of the siTCR vectors.

Discussion

In our previous study, we developed a novel siTCR retroviral vector for TCR gene therapy. This vector can express both siRNAs to silence endogenous TCRs and a codon-optimized, siRNA-resistant tumor antigen-specific TCR simultaneously. T cells transduced with these novel siTCR retroviral vectors could efficiently express the introduced TCR while reducing the expression of the endogenous TCR and enhancing the antigen-specific lysis of target cells at relatively low proviral copy numbers. We also demonstrated the remarkable advantages of TCR gene therapy using the siTCR retroviral vector in terms of enhancing the anti-leukemia effect in a mouse model.[23,24]

In gene therapy, retroviral vectors are the most commonly used gene transfer system for the stable transduction of various target cells.[31–33] The expression level of the transgenes can be enhanced by increasing the integrated vector copy number in the transduced cells. However, it is desirable to limit the vector copy numbers as much as possible, as this may reduce the risk of insertional mutagenesis caused by random genome insertion, even when using mature T cells instead of stem cells for safe TCR gene therapy. In an effort to improve the efficacy of TCR gene therapy using the siTCR retroviral vector, it is necessary to choose the best vector construct to achieve a higher expression level of transduced TCRs using the feasible strategy of expressing multiple genes in a single vector construct. Therefore, evaluating the efficacy of each retroviral vector with different viral titers using a precise evaluation method is indispensable for determining the most suitable and safe retroviral vector construct.

In general, the efficacy of a vector construct is based on the marker genes' expression level (which may also be influenced by vector constructs) and by the retroviral vector titer evaluated with other cells that cannot reflect the accurate transduction efficiency in the PBMCs. In this study, as in our previous study, we adopted an evaluation system based on the proviral copy number of the transduced PBMCs, reflecting the actual retroviral titer to precisely evaluate the usefulness and safety of each vector.[23] To increase the expression of TCRs, we first developed the retroviral vector backbone pMS3, which can achieve a higher expression of transgenes at a lower vector copy number than pMS can, and demonstrated the increase in MAGE-A4–specific TCR expression on the cell surface (**Supplementary Figure S1**). Among the strategies for expressing multiple genes from a single vector, internal ribosomal entry site and an additional internal promoter is likely to produce differing amounts of the encoded proteins. Therefore, the 2A peptide has been widely adopted for TCR gene therapy because of its comparatively stoichiometric expression of both TCRα and β chains. The 2A peptide allows multiple proteins to be encoded as a single polyprotein

and dissociates into each protein through a mechanism of ribosomal skipping. We demonstrated that by using the T2A peptide we could increase the RNA expression level of introduced TCRs (data not shown), resulting in the increased surface expression of WT1-specific TCRs. However, in the case of hTERT-specific TCRs, there was only a slight increase in the surface expression of ectopic TCRs; even the RNA expression levels and surface expression of the introduced TCRβ chain were increased significantly. In contrast and in spite of the lower expression level of RNA and the specific TCRβ chain, MS3-aPb-siTCR–transduced T cells were able to achieve much higher surface expression of ectopic TCRs when compared with vectors without siRNA expression (**Figure 1**). Our results clearly show the importance and advantage of the elimination of endogenous TCRs for efficient surface expression of ectopic TCRs using the siTCR technology.

In our previous study, which explored the best siTCR vector construct using an internal promoter, we generated many constructs that expressed siRNAs *via* short hairpin RNA transcription driven by pol II promoters and constructs expressing pri-microRNA (miRNA) structures based on human miRNA clustered on the human genome and transcribed as a single transcriptional unit.[34,35] After screening a variety of vector constructs that simultaneously expressed therapeutic TCRα and β chains and two siRNAs to silence endogenous TCRα and β, the construct expressing siRNAs using miRNA cluster sequences was found to be the most effective vector for expressing ectopic TCR in T cells (PM11 in the previous report).[23] Furthermore, we modified this construct to produce two pairs of siRNAs against each TCRα and β (PM11-w in the previous report),[23] and we demonstrated a more efficient expression of the TCRs on the cell surface with a low proviral copy number with this vector construct. To explore the second generation siTCR retroviral vector with increased expression of TCRs using the 2A peptide, we adopted a siRNA expression system using miRNA cluster sequences, just as we had used previously.[23] We compared several siTCR vector constructs expressing WT1-specific TCRs, although all siTCR vectors using the T2A peptide were able to achieve a higher ectopic TCR expression than the internal promoter type MS3-aPb-siTCR. Insertion of the siRNA expression unit in the upstream or downstream of TCR genes linked by the 2A peptide lowered the RNA expression of TCR chains. We succeeded in developing splice-typed siTCR retroviral vectors in which the siRNA expression unit was inserted upstream of the portion of intron and splice acceptor region from the human EF1-α (pSplice-siTCR), expressing pri-miRNA-like siRNA cluster sequences by RNA splicing between the splice donor and splice acceptor, processed into stem-loop form short hairpin RNA, and finally cleaved in the cytoplasm to produce siRNAs without a reduction in the therapeutic TCR RNA expression (**Figure 2**). We also demonstrated the superiority in ectopic TCR expression of Splice-siTCR vectors using MAGE-A4– and hTERT-specific TCRs (**Figures 3, 4**). Although the inclusion of the siRNA expression unit lowered the viral titers at some extent, Splice-siTCR retroviral vectors exerted the powerful effects. Another notable finding in our present study was the influence of the order of TCRα and β genes connecting the 2A peptide on the cell surface TCR expression. A potential disadvantage in the use of 2A peptides is the residual amino acids left on the C terminus of the first protein, which may affect the activity and expression of the protein and may cause an immune response to the transduced cells. Although several groups have reported the TCR gene transfer using the 2A peptide, the effect of the residual amino acids on the expression and function of ectopic TCRs has not been fully investigated. We have demonstrated that "b2Aa" was always superior to "a2Ab" in the specific TCR expression on the cell surface with all TCRs tested in this study (**Figure 3**) and with six other distinct TCRs (data not shown), indicating that the residual amino acids on the C terminus of TCRα chain affect the expression of introduced TCRs. We have also evaluated the effect of residual amino acids on the C terminus of TCRα and β chains using TCRα- or TCRβ-expressing retroviral vectors with or without insertion of 2A peptide sequences between CDS and stop codon, and found the residual amino acids decreased the RNA and protein expression of both TCRα and β chains, however, the expression of TCRα seemed to be lowered more than that of TCRβ (data not shown). Although the mechanism of the difference in TCR expression by the order of TCRs was not clear, the residual amino acids on the C terminus of TCRα chain affect the expression of introduced TCRs more than that of TCRβ chain (**Figures 3, 4**). In TCR gene-modified T cells, the expression of therapeutic TCR on the cell surface involves two steps, the formation of the TCRαβ heterodimer and the association of CD3 molecules. As we have demonstrated with the universal effect of the siTCR technology without the dependency of TCR variations, the silencing of endogenous TCR could improve the correct pairing of transduced TCRαβ heterodimers by reducing the formation of mixed TCRs in the first step and facilitate the formation of therapeutic TCRs-CD3 complexes by reducing endogenous TCR dimers and mixed TCR dimers in the second step, regardless of TCR variation. In contrast, the addition of a disulfide bond by cysteine modification can improve the correct TCR pairing, resulting in the reduced formation of mixed TCRs in the first step. It cannot, however, improve the formation of TCR-CD3 complexes in the second step, and therefore the cysteine modification may have little effect on the "strong" TCR dimers in the first step or the "weak" TCR dimers in the second step. As we have shown in this study, the combination of the siTCR technology and cysteine modification with different sites of action worked exceedingly well for improving ectopic TCR expression with WT1- and hTERT-specific TCRs (**Figures 4, 5**). Thus, the combination of several strategies to reduce TCR mispairing may be a powerful tool for TCR gene therapy.

In summary, we demonstrated the feasibility of our novel siTCR technology for TCR gene therapy with its universal effects without the dependency of TCR variations, enhancing the surface expression of therapeutic TCRs at low proviral copy numbers, which may reduce the risk of mutagenesis and TCR mispairing, which in turn may cause the risk of autoimmunity. This novel TCR gene therapy approach using siTCR retroviral vectors may be a promising technique in terms of efficacy and safety for patients with malignancies and/or viral infections.

Materials and methods

Cell lines and PBMCs. The HEK293T and PG13 cell lines were cultured in Dulbecco's modified Eagle's medium

(Sigma-Aldrich, St Louis, MO) and supplemented with 10% fetal bovine serum, penicillin (100 U/ml), and streptomycin (100 mg/ml). The T2A24[36] cell lines were maintained in RPMI1640 (Sigma-Aldrich) with 10% fetal bovine serum, penicillin (100 U/ml), and streptomycin (100 μg/ml). The study was approved by the Ethics Committee of Takara Bio (Shiga, Japan). The PBMCs were isolated from healthy donors (who gave their informed consent) by leukapheresis, followed by Ficoll-Isopaque density centrifugation. The PBMCs were cultured in GT-T503 (Takara Bio) and supplemented with 1% autologous plasma, 0.2% HSA, 2.5 mg/ml fangizon (Bristol-Myers Squibb, New York, NY), and 600 IU/ml interleukin-2.

Construction of TCR gene expression retroviral vectors. The HLA-A*2402-restricted MAGE-A4$_{143-151}$–specific TCRα and β genes were cloned from CD8+ CTL clone 2-28,[8,22,36] and the HLA-A*2402-restricted WT1$_{235-243}$–specific TCRα and β genes were cloned from CD8+ CTL clones TAK-1, as reported previously.[37–39] The HLA-A*2402-restricted hTERT$_{461-469}$–specific TCRα and β genes were cloned from CD8+ CTL clones[40] as described previously,[8] and TCRα and β were typed as TRAV29DV5/TRAJ34/TRAC and TRBV20-1/TRBJ2-1/TRBC2. The MAGE-A4–specific TCRα and β cDNA sequences were fully codon-modified by GeneArt (Regensburg, Germany), and only the C region of the WT1- and hTERT-specific TCRα and β genes was codon-optimized to escape interference from siRNAs. We used the pMS or pMS3 retroviral vector backbones to express TCRs, pMS-aPb and pMS3-aPb retroviral vectors containing both codon-optimized TCRα and β, while the murine stem cell virus LTR drove the expression of the TCRα gene, and the mouse phosphoglycerate kinase promoter drove the expression of the TCRβ gene (**Supplementary Figure S1a**, **Figures 1a,2a**). The retroviral vectors pMS-a2Ab and pMS3-a2Ab were constructed using InFusion cDNA cloning technology (Clontech, Mountain View, CA) with the following configuration: TCRα chain, SGSG-linker peptide, T2A peptide, and TCRβ chain (**Supplementary Figure S1a**, **Figures 1a,2a,3a**). For siTCR retroviral vectors, the siRNA expression unit using cluster sequences of human pri-miRNA (miR-17-20), in which the mature miRNA sequences were replaced by four siRNA sequences to knockdown the endogenous TCRα and β,[23] was inserted into the retroviral vectors encoding codon-optimized TCRs (**Figures 1a,2a,3a**).

Retroviral vector production and retroviral transduction. The ecotropic and vesicular stomatitis virus G-pseudotyped retroviruses were transiently obtained by conventional methods using HEK293T cells. The PG13 cells were transduced with transiently produced ecotropic retroviruses to produce GaLV-pseudotyped retroviruses. The cells were transduced using the RetroNectin-bound virus infection method, in which retroviral solutions were preloaded onto RetroNectin- (Takara Bio) coated plates, centrifuged at 2,000*g* for 2 hours at 32 °C, and then rinsed with phosphate-buffered saline. The cells were applied to the virus-preloaded plate. The PBMCs were stimulated with 30 ng/ml OKT-3 (Janssen pharmaceuticals, Titusville, NJ) and 600 IU/ml of interleukin-2 on day 0, and the gene transfer was performed twice on days 3 and 4.

Flow cytometry analysis. We double-stained the transduced PBMCs with FITC-conjugated anti-CD8 Ab (Becton Dickinson, San Jose, CA) and PE-conjugated MAGE-A4$_{143-151}$/HLA-A*2402 tetramers (Ludwig Institute for Cancer Research, New York, NY), WT1$_{235-243}$/HLA-A*2402 tetramers (MBL, Aichi, Japan), and hTERT$_{461-469}$/HLA-A*2402 tetramers (provided by Mie University, Mie, Japan). The hTERT-specific TCR-transduced PBMCs were double-or triple-stained with PE-conjugated hTERT$_{461-469}$/HLA-A*2402 tetramers, FITC-conjugated anti-human TCR Vβ2 Ab (Beckman Coulter, Brea, CA), and PerCP-conjugated anti-CD8 Ab (Becton Dickinson). The stained cells were analyzed using a FACSCant II Flow Cytometer (Becton Dickinson). The WT1 tetramer-positive cells were sorted using FACSAria III (Becton Dickinson), and the MAGE-A4 tetramer-positive cells were collected using MACS Anti-PE Multisort Kit (Miltenyi Biotec, Auburn, CA).

Measurement of the proviral copy number of retrovirus-transduced PBMCs. The genomic DNA from the transduced PBMCs was purified, and the average proviral copy number per cell was quantified using the Cycleave PCR Core Kit (Takara Bio) and the Proviral Copy Number Detection Primer Set (Takara Bio).

TCR RNA quantification. The quantification of TCR RNAs was performed as described previously.[23] Briefly, the total RNA was extracted, and quantitative reverse transcription-PCR was performed using the SYBR PrimeScript RT-PCR Kit (Takara Bio) with the primer sets specific to the TCR C regions. Glyceraldehyde-3-phosphate dehydrogenase was used for normalization.

Intracellular cytokine staining. In 96-well plate, 1 × 10^5 cells of PBMCs transduced with retroviral vectors expressing MAGE-A4– or WT1-specific TCRs were mixed with 1 × 10^5 cells of T2A24 cells pulsed with 20 ng/ml of MAGE-A4$_{143-151}$ or WT1$_{235-243}$ peptides for 1 hour. After 6 hours of incubation, cells were stained with FITC-conjugated anti-CD8 Ab, then permeabilized in the cytoplasmic membrane using IntraPrep reagents (Beckman Coulter) and stained with PE-conjugated IFNγ Ab (Beckman Coulter) and APC-conjugated TNFα Ab (eBioscience, San Diego, CA), according to the manufacturer's protocol. The stained cells were analyzed using a FACSCant II Flow Cytometer.

Genomic PCR of proviral vector in PG13 producer cell lines. The genomic DNA from the PG13 producer cell lines was purified, and PCR was performed to amplify proviral DNA using F primer (5′-TCTGTGTCTGTCCGATTG-3′) and R primer (5′-CTACAGGTGGGGTCTTTCA-3′).

Supplementary Material

Figure S1. The influence of vector backbones on transgene expression.

Acknowledgments. We thank Yuki Orito (Mie University) for generously providing tetramers, Kanako Isoe (Takara Bio), Nozomi Iwase (Takara Bio), and Ayumi Kawamura (Mie University) for expert technical contributions. This work was done in Shiga, Japan. The authors declared no conflict of interest.